

Modified Salicylanilide and 3-Phenyl-2*H*-benzo[*e*][1,3]oxazine-2,4(3*H*)-dione Derivatives as Novel Inhibitors of Osteoclast Differentiation and Bone Resorption

Chun-Liang Chen,^{†,‡} Fei-Lan Liu,[§] Chia-Chung Lee,^{†,‡} Tsung-Chih Chen,^{†,‡} Ahmed Atef Ahmed Ali,^{‡,||} Huey-Kang Sytwu,^{‡,⊥} Deh-Ming Chang,^{*,‡,§} and Hsu-Shan Huang^{*,†,‡,‡,⊥}

[†]Graduate Institute of Cancer Biology and Drug Discovery, College of Medical Science and Technology, Taipei Medical University, Taipei 110, Taiwan ROC

[‡]Graduate Institute of Life Sciences, National Defense Medical Center, Taipei 114, Taiwan ROC

[§]Rheumatology/Immunology/Allergy, Taipei Veterans General Hospital, Taipei 112, Taiwan ROC

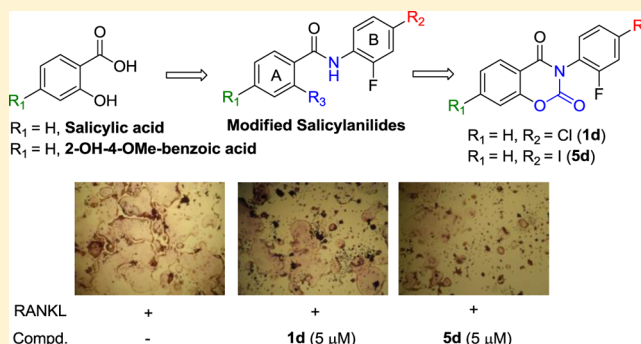
^{||}Taiwan International Graduate Program, Molecular and Cell Biology Program, Institute of Molecular Biology, Academia Sinica, Taipei 115, Taiwan ROC

[⊥]Department and Graduate Institute of Microbiology and Immunology, National Defense Medical Center, Taipei 114, Taiwan ROC

^{*}School of Pharmacy, National Defense Medical Center, Taipei 114, Taiwan ROC

Supporting Information

ABSTRACT: Inhibition of osteoclast formation is a potential strategy to prevent inflammatory bone resorption and to treat bone diseases. In the present work, the purpose was to discover modified salicylanilides and 3-phenyl-2*H*-benzo[*e*]-[1,3]oxazine-2,4(3*H*)-dione derivatives as potential antiosteoclastogenic agents. Their inhibitory effects on RANKL-induced osteoclastogenesis from RAW264.7 cells were evaluated by TRAP stain assay. The most potent compounds, **1d** and **5d**, suppressed RANKL-induced osteoclast formation and TRAP activity dose-dependently. The cytotoxicity assay on RAW264.7 cells suggested that the inhibition of osteoclastic bone resorption by these compounds did not result from their cytotoxicity. Moreover, both compounds downregulated RANKL-induced NF- κ B and NFATc1 in the nucleus, suppressed the expression of osteoclastogenesis-related marker genes during osteoclastogenesis, and prevented osteoclastic bone resorption but did not impair osteoblast differentiation in MC3T3-E1. Therefore, these modified salicylanilides and 3-phenyl-2*H*-benzo[*e*][1,3]oxazine-2,4(3*H*)-diones could be potential lead compounds for the development of a new class of antiresorptive agents.



INTRODUCTION

Bone is a dynamic tissue that is constantly undergoing a repair and renewal process termed bone remodeling.¹ Bone-resorbing cells (osteoclasts) together with bone-forming cells (osteoblasts) play the pivotal roles in bone remodeling.² Generalized bone loss with reduced mineral density, bone destruction, and imbalance of bone remodeling are pathological hallmarks of osteoporosis, inflammatory joint disease, and rheumatoid arthritis (RA).^{3–5} Bone resorption is dependent on a cytokine known as receptor activator of nuclear factor κ B ligand (RANKL), and RANKL inhibitors can prevent focal bone loss that occurs in animal models of RA.⁶

Osteoclasts originate from the fusion of mononuclear progenitors of the monocyte/macrophage hematopoietic lineage that resorb bone in the presence of RANKL.^{2,7} RANKL is a member of the tumor necrosis factor (TNF) superfamily produced mainly by the osteoblasts, which

regulates the process of osteoclastogenesis and maintains the survival of mature osteoclasts.⁸ When RANKL binds to the cell-surface receptor RANK, the initiation of signal transduction triggers downstream signaling cascades, including the NF- κ B, mitogen-activated protein kinase, c-fos, and nuclear factor of activated T cells c1 (NFATc1) pathways that contribute to RANKL-induced osteoclastogenesis.^{9,10} Among these transcription factors, NFATc1 is a critical target for controlling excessive osteoclastogenesis. Agents that can suppress NFATc1, such as FK506 and cyclosporin A, have been approved for the inhibition of osteoclastogenesis.^{11,12} On the basis of promoter analyses, some osteoclast-specific genes, such as the tartrate-resistant acid phosphatase (*TRAP*), *cathepsin K*, *MMP-9*, and dendritic cell-specific transmembrane protein (*DC-STAMP*)

Received: June 27, 2014

Published: September 9, 2014

genes, are directly regulated by NFATc1 and required for bone resorptive activity of osteoclasts and cell–cell fusion during osteoclast development.^{10,13–16} Further, *NFATc1* is a critical target gene of NF- κ B in the early phase of osteoclastogenesis.¹² The importance of *NFATc1* in osteoclastogenesis is also demonstrated by the in vitro observation that *NFATc1*^{-/-} embryonic stem cells exhibit a defect in osteoclastogenesis.^{12,14} Also, *c-fos* expression is essential for osteoclastogenesis in response to RANKL stimulation, as *c-fos*-deficient mice were found to develop osteopetrosis due to a lack of osteoclasts.¹⁷ Through these mechanisms of RANKL-induced osteoclastogenesis and bone resorption, the RANK signaling pathway provides molecular targets for the development of therapeutics to treat RA and other bone-related diseases.¹⁸ Thus, searching for powerful small-molecule osteoclastogenesis inhibitors that can suppress RANKL signaling and regulate the activity of osteoclasts still holds great promise for the development of antiresorptive agents.

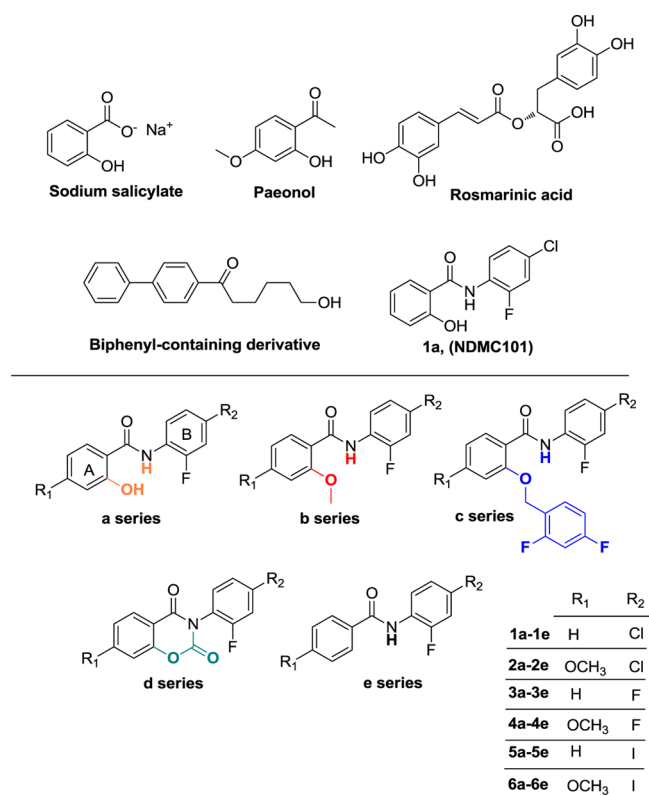
Furthermore, synthetic analogues of bisphosphonates are currently the most important and effective antiresorptive drugs, but they have been shown to cause gastrointestinal tract side effects, osteonecrosis of the jaw, and renal toxicity and to lead to the suppression of bone turnover as well as a reduction in bone quality after long-term treatment.^{19–21} Hence, numerous osteoclastogenesis inhibitors have been developed, including natural product and synthetic small molecules such as sodium salicylate, paeonol, rosmarinic acid, biphenyl-containing derivatives, and salicylanilides (Scheme 1).^{22–27} In addition, salicylanilides were found to be inhibitors of interleukin production and to show potent antitumor activity.^{28,29} As part of an effort to profile potential osteoarthritis therapeutics, we previously reported that a salicylanilide core scaffold

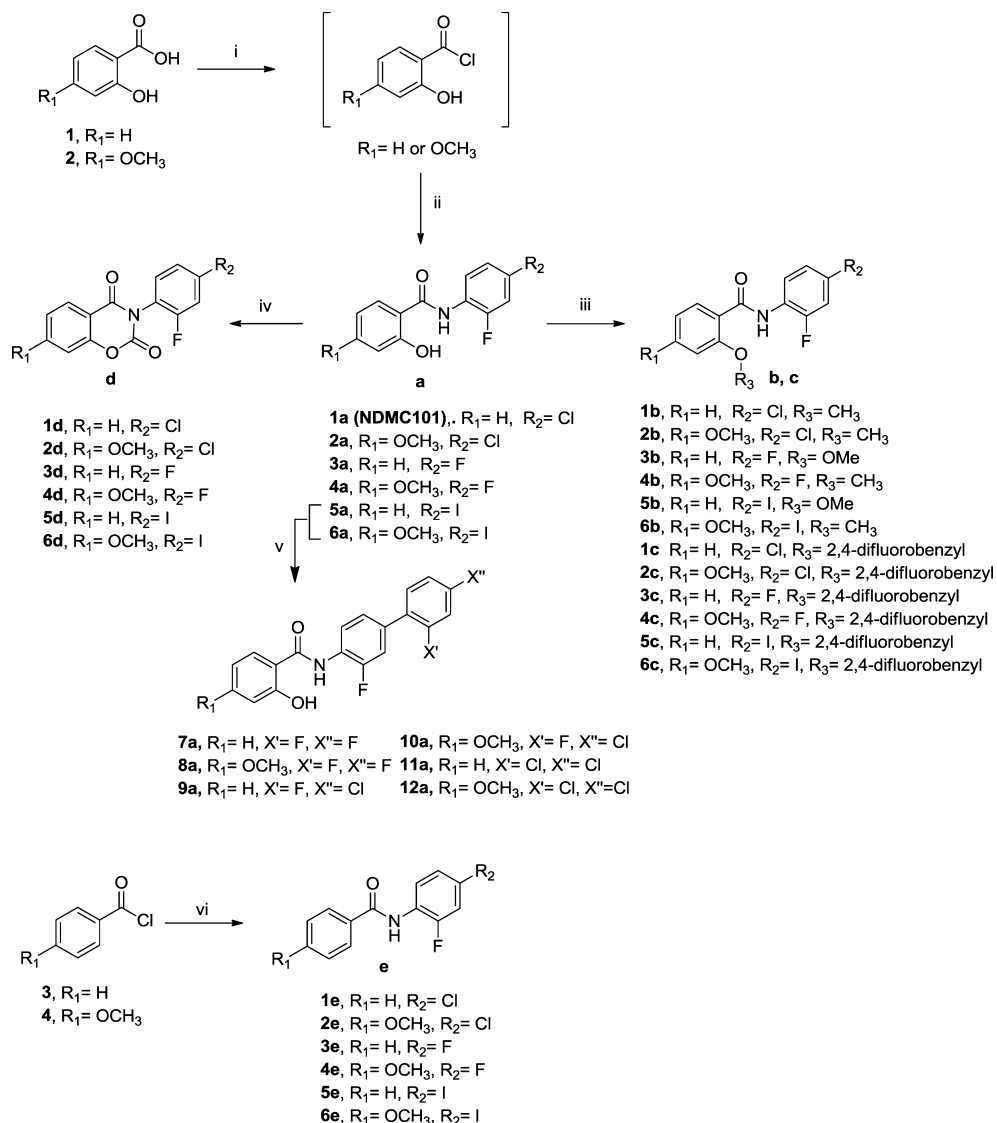
derivative (**HS-Cf**) inhibits TNF- α -induced interferon regulatory factor-1 in porcine chondrocytes.³⁰ We also found that the salicylanilide derivative NDMC101 (**1a**) inhibits RANKL-induced osteoclast differentiation by suppressing NFATc1 and NF- κ B activity and ameliorates paw-swelling inflammation of bones in collagen-induced arthritic mice.²⁵ On the basis of these findings, salicylanilide-derived small molecules could be lead structures that warrant further optimization.

In the present work, we developed a series of novel synthetic inhibitors of RANKL-induced osteoclastogenesis. We designed and synthesized a series of small molecules containing various core scaffolds such as salicylanilide analogues (series **a**, **b**, and **c**), 3-phenyl-2*H*-benzo[*e*][1,3]oxazine-2,4(3*H*)-dione analogues (series **d**), and *N*-phenylbenzamide analogues (series **e**). These compounds were classified as series **a–e** according to the substituent at the 2-position of benzene ring A of the salicylanilide core structure. For each series, there are six different member compounds distinguished by the substituent groups of benzene rings A and B (Scheme 1). Furthermore, since some biphenyl-containing derivatives inhibit osteoclastic bone resorption by inducing osteoclast apoptosis and inhibiting osteoclast formation,^{26,27,31} we were particularly interested in replacing the iodine atom in **5a** and **6a** with a phenyl group, affording compounds **7a–12a**. To characterize the biological activities of these synthetic compounds, we evaluated their effects on RANKL-induced osteoclastogenesis from osteoclast precursor cells (RAW264.7) by the TRAP stain assay. Using this screen, we identified 3-phenyl-2*H*-benzo[*e*][1,3]oxazine-2,4(3*H*)-dione derivatives **1d** and **5d**, which can effectively inhibit RANKL-induced osteoclastogenesis. On the basis of this preliminary screening, we also constructed structure–activity relationships (SARs) of these synthetic compounds according to the inhibition of RANKL-induced osteoclastogenesis. Within an in vitro screening research program to discover these inhibitors, our results showed that hydroxyl or halogen groups on salicylanilide and 3-phenyl-2*H*-benzo[*e*][1,3]oxazine-2,4(3*H*)-dione derivatives could be the key elements related to the inhibition activity.

On the basis of these results, we considered the most potent compounds **1d** and **5d** to inhibit RANKL-induced osteoclast formation and antiresorptive effects by suppressing osteoclastogenesis-related genes, reducing NFATc1 levels, and blocking NF- κ B nuclear translocation. Furthermore, osteogenesis is a vital process for the maintenance of skeleton and bone formation in terms of bone development.³² Mature osteoblastic cells exhibit their osteoblastic characteristics during osteogenesis, such as alkaline phosphatase (ALP) production and deposition of extracellular matrix (ECM) on the substrate, which are subsequently mineralized.³³ Currently, the effects of salicylanilides and 3-phenyl-2*H*-benzo[*e*][1,3]oxazine-2,4(3*H*)-dione derivatives on osteogenesis are still unknown. Hence, we investigated the effects of compounds **1a**, **1d**, and **5d** on osteoblastic differentiation using MC3T3-E1 mouse calvaria-derived osteoprogenitor cells, which are widely used as a model to study osteogenic development.^{34,35} We found that **1a**, **1d**, and **5d** showed no significant effects on osteoblastic differentiation markers such as the ALP activity and mineral deposition in MC3T3-E1 cells. This demonstrates that these novel modified salicylanilides and 3-phenyl-2*H*-benzo[*e*][1,3]oxazine-2,4(3*H*)-dione derivatives could be inhibitors of RANKL-induced osteoclastogenesis without affecting osteoblast differentiation. Thus, these structures could be promising lead compounds that warrant further structure optimization

Scheme 1. Chemical Structures of Osteoclast Inhibitors and Classification of Our Synthetic Compounds



Scheme 2. Synthesis of Modified Salicylanilide and 3-Phenyl-2*H*-benzo[*e*][1,3]oxazine-2,4(3*H*)-dione Derivatives^a

^aReagents and conditions: (i) thionyl chloride, THF, reflux; (ii) aniline series, THF, reflux; (iii) iodomethane or 2,4-difluorobenzyl bromide, K₂CO₃, acetone, reflux; (iv) methyl chloroformate, pyridine, reflux; (v) K₂CO₃, Pd(OAc)₂, PPh₃, toluene, reflux; (vi) aniline series, TEA, THF, room temperature.

and SAR studies to present novel drugs for the treatment of bone diseases.

CHEMISTRY

The synthetic routes to obtain the target modified salicylanilide derivatives by condensation reactions of salicylic acid and 2,4-disubstituted anilines are outlined in Scheme 2. Commercially available salicylic acid (**1**) or 2-hydroxy-4-methoxybenzoic acid (**2**) was transformed into the corresponding acid chloride using excess thionyl chloride, and the acid chloride was reacted with the substituted anilines to give the corresponding compounds **1a–6a**. In order to identify the role of the hydroxyl group in the activity of salicylanilide, 2-methoxybenzanilide (**1b–6b**), 2-(2,4-difluorobenzyl)oxybenzanilide (**1c–6c**), and *N*-phenylbenzamide (**1e–6e**) derivatives were prepared. Compounds **1b–6b** and **1c–6c** were obtained from the reaction of **1a–6a** with iodomethane or 2,4-difluorobenzyl bromide through nucleophilic substitution. The *N*-phenylbenzamide derivatives **1e–6e** were obtained from the aniline series by reaction with

benzoyl chloride or 4-methoxybenzoyl chloride. Then the modified salicylanilides **1a–6a** were cyclized and converted to 3-phenyl-2*H*-benzo[*e*][1,3]oxazine-2,4(3*H*)-dione derivatives **1d–6d** by treatment with methyl chloroformate in pyridine. This reaction was based on a literature report describing the cyclization reaction of salicylanilides.³⁶ Furthermore, the biphenyl-containing derivatives **7a–12a** were prepared by palladium-catalyzed Suzuki–Miyaura coupling reactions between various 2,4-disubstituted boronic acids and iodine-atom-containing salicylanilide **5a** or **6a**. The purities of all final compounds (>95%) were determined by HPLC. The structures of the synthesized compounds were determined by ¹H and ¹³C NMR spectroscopy and high-resolution mass spectrometry (HRMS).

RESULTS AND DISCUSSION

Effects of the Synthetic Compounds on RANKL-Induced Osteoclast Differentiation. After the construction of a series of synthetic compounds, we evaluated their

inhibitory activities against RANKL-induced osteoclast differentiation from RAW264.7 cells. As shown in Table 1, several analogues caused more than 50% inhibition of RANKL-induced osteoclastogenesis at 10 μM as determined by the TRAP assay using **1a** as a positive control. According to previous studies, the starting materials (salicylic acid and 2-hydroxy-4-methoxybenzoic acid) revealed inhibition of venom-induced inflam-

Table 1. Effects of Compounds on Cell Viability and RANKL-Induced Osteoclast Differentiation from RAW264.7 Cells

compd	cell viability ^a		osteoclastogenesis ^b
	survival rate at 10 μM (%)	CC ₅₀ (μM)	TRAP ⁺ MNCs at 10 μM (%)
1^c	99.8 \pm 12.2	>40	99.8 \pm 7.5
2^c	99.4 \pm 7.6	>40	79.6 \pm 8.3
1a	93.0 \pm 3.1	23.2 \pm 0.6	49.4 \pm 5.4
1b	101.8 \pm 4.5	>40	86.0 \pm 9.9
1c	107.2 \pm 4.5	>40	74.6 \pm 6.2
1d	97.9 \pm 2.0	26.5 \pm 1.0	19.7 \pm 4.9
1e	105.2 \pm 7.4	>40	77.9 \pm 6.4
2a	103.0 \pm 2.8	32.3 \pm 4.9	23.8 \pm 3.4
2b	52.9 \pm 2.8	13.6 \pm 1.2	60.2 \pm 3.6
2c	107.3 \pm 4.4	>40	68.7 \pm 4.6
2d	100.5 \pm 2.4	>40	36.0 \pm 1.8
2e	105.5 \pm 1.2	>40	100.4 \pm 4.0
3a	76.1 \pm 6.3	38.4 \pm 2.7	85.2 \pm 11.5
3b	108.5 \pm 4.0	>40	89.1 \pm 5.1
3c	101.1 \pm 3.2	>40	97.6 \pm 6.0
3d	88.8 \pm 0.6	>40	82.5 \pm 8.4
3e	105.2 \pm 9.4	>40	75.2 \pm 8.1
4a	89.7 \pm 4.0	>40	74.9 \pm 7.4
4b	102.5 \pm 9.3	>40	93.0 \pm 7.7
4c	106.0 \pm 8.8	>40	66.2 \pm 8.1
4d	90.9 \pm 5.4	>40	67.5 \pm 5.0
4e	101.8 \pm 4.9	>40	73.3 \pm 8.1
5a	96.7 \pm 5.0	23.3 \pm 0.3	70.6 \pm 13.9
5b	95.4 \pm 5.4	>40	106.6 \pm 6.7
5c	85.0 \pm 4.2	32.6 \pm 3.8	85.5 \pm 8.5
5d	91.4 \pm 3.4	23.6 \pm 0.4	1.8 \pm 2.4
5e	105.2 \pm 3.4	>40	76.8 \pm 10.7
6a	94.4 \pm 4.8	27.6 \pm 2.0	39.4 \pm 9.3
6b	95.0 \pm 1.7	>40	92.4 \pm 9.8
6c	104.2 \pm 9.3	36.8 \pm 5.9	51.3 \pm 6.6
6d	103.2 \pm 9.0	30.1 \pm 0.9	44.4 \pm 9.4
6e	91.4 \pm 9.2	32.8 \pm 7.3	89.3 \pm 6.9
7a	102.5 \pm 7.6	28.6 \pm 3.1	100.1 \pm 6.2
8a	64.5 \pm 7.3	26.3 \pm 3.7	50.1 \pm 11.5
9a	90.9 \pm 3.1	27.2 \pm 3.8	84.8 \pm 7.4
10a	44.5 \pm 6.6	N.T. ^d	60.6 \pm 5.8
11a	105.1 \pm 5.7	29.8 \pm 5.0	91.2 \pm 7.9
12a	102.5 \pm 6.0	>40	92.5 \pm 12.1

^aCC₅₀ is the concentration of the tested compound required to inhibit cell viability by 50% of the mean ($N = 3$). ^bTo induce differentiation of murine RAW 264.7 cells, the cells were cultured in α -MEM medium containing 10% FBS and 100 ng/mL RANKL with or without the tested compound (10 μM) for 4 days. TRAP-positive multinucleated cells (TRAP⁺ MNCs) having five or more nuclei were considered as osteoclasts. RANKL-induced osteoclast differentiation is shown as relative activity (% of the compound-treated group relative to the RANKL-treated group). ^cSalicylic acid (**1**), 2-hydroxy-4-methoxybenzoic acid (**2**). ^dN.T. = not tested.

mation or osteoclast differentiation,^{22,37} but they showed less inhibition against RANKL-induced osteoclast differentiation at 10 μM . Herein, the SAR study was focused on the effects of the side chains on the aromatic ring. Among our synthetic salicylanilide derivatives (**1a–6a**), it was noted that the osteoclast inhibitory activities of the 4-iodo-substituted (**5a**, **6a**) and 4-chloro-substituted (**1a**, **2a**) compounds were more potent than those of the 2-fluoro-substituted (**3a**, **4a**) compounds. These observations revealed that the halogen substituent (inhibitory activities: Cl and I > F) at the 4-position on benzene ring B of the salicylanilide may modulate the inhibition of osteoclastogenesis. We also found that the inhibition of osteoclastogenesis was increased by introducing the methoxy substituent group at the 4-position of the benzene ring A compared with the corresponding H-substituted compounds (inhibitory activities: **2a** > **1a**; **4a** > **3a**; **6a** > **5a**) (Table 1). In addition, replacement of the 2-hydroxyl group of the salicylanilide with a methoxy group (**1b–6b**) or a 2-(2,4-difluorobenzyl)oxy group (**1c–6c**) led to the loss of osteoclastogenesis inhibitory activity. This suggests that the 2-hydroxyl moiety of salicylanilide derivatives could be a key pharmacophore for inhibition of osteoclast formation. We also observed that the absence of the hydroxyl group at the 2-position of the *N*-phenylbenzamide derivatives (**1e–6e**) led to loss of potency against RANKL-induced osteoclastogenesis. In addition, there are some reports indicating that biphenyl-containing derivatives can inhibit osteoclastic bone resorption by inducing osteoclast apoptosis and inhibiting osteoclast formation.^{26,27} However, our compounds with a biphenyl structure (**7a–12a**) were less potent than **1a** at a concentration of 10 μM . Next, the antiosteoclastogenic effects of 3-phenyl-2*H*-benzo[*e*][1,3]oxazine-2,4(3*H*)-dione derivatives (**1d–6d**) were evaluated. Among them, compounds **1d** and **5d** were the most potent inhibitors among our synthetic compounds against RANKL-induced osteoclast formation. Hence, **1d** and **5d** were selected as potential structures for further pharmacological evaluations. The SARs and the key pharmacophore of our synthetic compounds for osteoclastogenesis inhibition are described in Scheme 3.

In order to confirm that the antiosteoclastogenic effects of compounds are not attributable to cellular toxicity, we investigated the effect of the compounds on cell viability using RAW264.7 osteoclast progenitor cells by performing the MTT assay (Table 1). The results showed that all of the compounds had slight or no effect on cell viability of RAW264.7 cells at a concentration of 10 μM [survival rate >85% except for **2b** (52.9%), **3a** (76.1%), **8a** (64.5%), and **10a** (44.5%)]. Furthermore, the concentrations of compounds required to inhibit cell viability by 50% of the mean (CC₅₀) were determined. Interestingly, all of the synthetic analogues had higher CC₅₀ values than **1a** (23.2 μM) except for **2b** (13.6 μM). These results suggest that the antiosteoclastogenic activities of these compounds are not due to their cytotoxicities toward osteoclast precursor cells.

Inhibitory Effects of 1d and 5d against RANKL-Induced Osteoclast Differentiation. Compounds **1d** and **5d** were the most potent inhibitors among all of the tested compounds. Both compounds reduced the number of red TRAP-positive osteoclasts and decreased the size of multinucleated osteoclasts significantly in a dose-dependent manner (Figure 1). Compounds **1d** (Figure 2A) and **5d** (Figure 2E) also showed no effect on the cell viability of osteoclast progenitor cells at 5 and 10 μM (Figure 2B,F). Furthermore, in

Scheme 3. SARs and the Key Pharmacophore for Osteoclastogenesis Inhibition

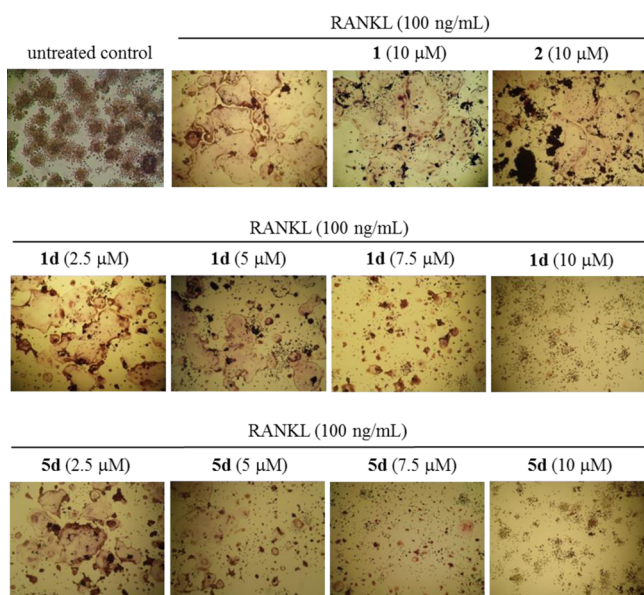
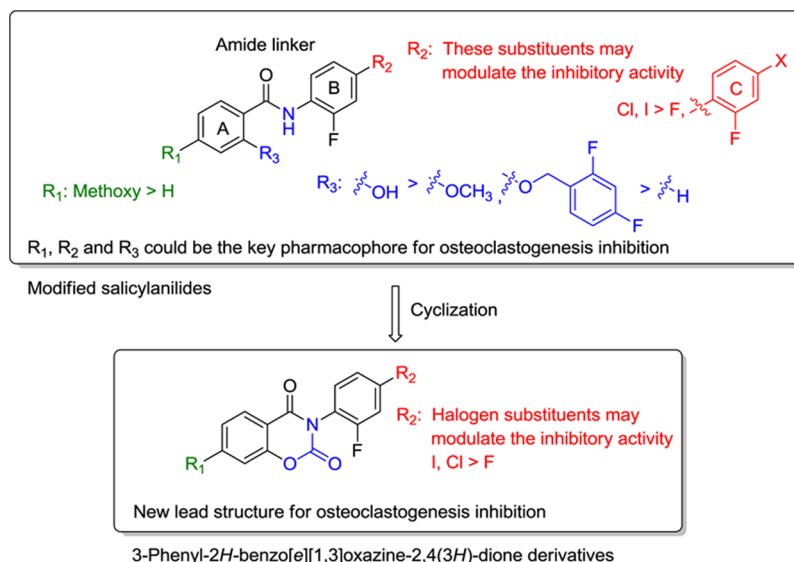


Figure 1. Effects of compounds **1d** and **5d** on RANKL-induced osteoclast differentiation from RAW264.7 cells. RAW264.7 cells were cultured with the tested compounds in the presence of RANKL (100 ng/mL) for 4 days. Cells were then fixed and stained for TRAP. The TRAP-positive multinucleated cells containing more than five nuclei were visualized by light microscopy. [Salicylic acid (**1**); 2-hydroxy-4-methoxybenzoic acid (**2**).]

comparison with the RANKL-treated group, compound **1d** decreased the percentage of TRAP-positive multinucleated cells generated (percentage of the **1d**-treated group relative to the RANKL-treated group), with 74.6% at 5 μM and 45.9% at 7.5 μM (Figure 2C). Also, TRAP-positive multinucleated cells were significantly reduced after treatment with compound **5d** (Figure 2G) (74.1% at 2.5 μM , 49.1% at 5 μM , and 29.1% at 7.5 μM). In addition, the IC_{50} values of the compounds on RANKL-induced osteoclastogenesis from RAW264.7 cells were calculated. The IC_{50} values of **1d** and **5d** for TRAP-positive multinucleated osteoclast formation were 7.1 and 4.9 μM , respectively (Table 2). To test whether the compounds inhibited the activity of osteoclasts, the inhibitory effects of

1d and **5d** on RANKL-induced TRAP activity were determined. Both compounds were found to dose-dependently suppress RANKL-induced TRAP activity (Figure 2D,H) with IC_{50} values of 10.6 and 7.3 μM , respectively (Table 2). On the basis of these results, we conclude that our new 3-phenyl-2H-benzo[e][1,3]oxazine-2,4(3H)-dione derivatives **1d** and **5d** are potent inhibitors of RANKL-induced osteoclastogenesis.

Effects of 1d and 5d on the Expression of NFATc1-Mediated Genes and Osteoclastogenesis-Related Marker Genes during RANKL-Induced Osteoclast Development. Osteoclast formation is executed directly by the upregulation of specific genes such as *NFATc1* and *c-fos* in response to the RANKL–RANK interaction.⁶ Herein we examined the effects of **1d** and **5d** on RANKL-induced regulation of *NFATc1* and *c-fos* expression for 24 or 48 h using *gapdh* as an internal control (Figure 3). Increased levels of *NFATc1* and *c-fos* mRNA were observed after RANKL stimulation, but expression of both *NFATc1* and *c-fos* were significantly decreased by treatment with **1d** and **5d**. The expression of *DC-STAMP* is rapidly induced by RANKL, regulated by *NFATc1*, and related to cell–cell fusion during osteoclast development.^{15,16} Our results revealed that the *DC-STAMP* mRNA level increased in the presence of RANKL and decreased upon treatment with **1d** and **5d** (Figure 3). Moreover, the TRAP enzyme is abundantly expressed by osteoclasts and involved in bone resorption.³⁸ Cathepsin K is a matrix-degrading enzyme that degrades type-I collagen and collagenous bone matrix.^{39,40} MMP-9 is one of the matrix metalloproteases that initiates bone degradation by removing the bone-lining collagen and involves in the invasion of osteoclasts.^{41,42} As shown in Figure 3, the mRNA expression levels of *TRAP*, *cathepsin K*, and *MMP-9* increased in response to RANKL, but expressions of these mRNA were significantly suppressed by **1d** and **5d** in a concentration-dependent manner. On the basis of these results, we conclude that compounds **1d** and **5d** may inhibit osteoclast differentiation through inhibition of RANKL-induced *NFATc1* and *c-fos* gene expression.

Effects of 1d and 5d on RANKL-Induced NF- κ B and NFATc1 Levels in the Nucleus. Activation of the transcription factor NF- κ B is important in osteoclastogenesis and

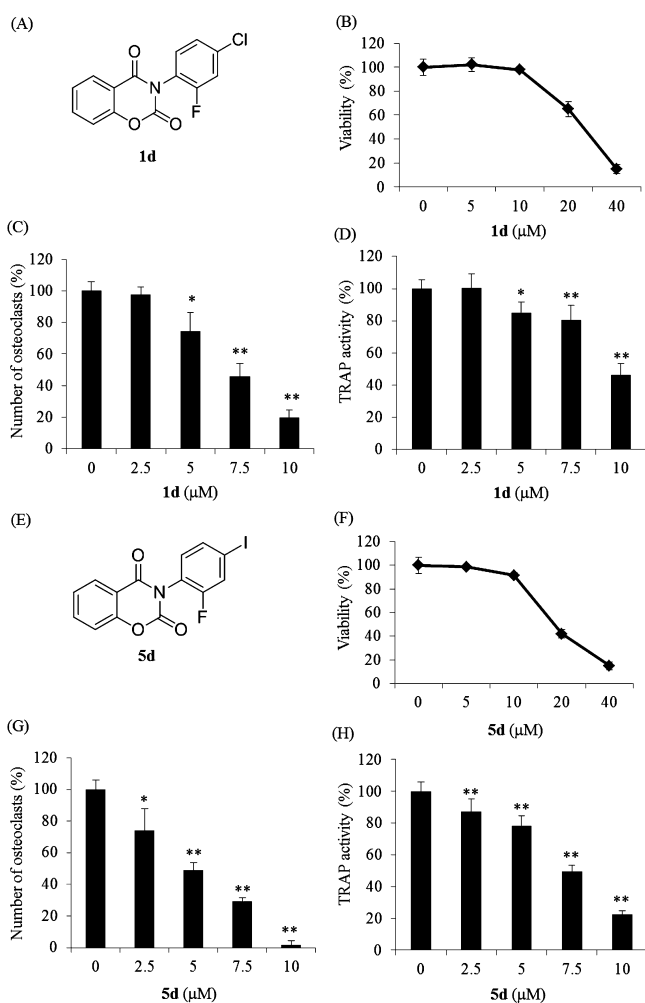


Figure 2. Inhibition of RANKL-induced osteoclast differentiation by compounds **1d** and **5d**. (A, E) Chemical structures of **1d** and **5d**. (B, F) Effects of compounds **1d** and **5d** (5–40 μM) on cell viability of RAW264.7 cells by MTT assay. (C, G) Compounds **1d** and **5d** reduced RANKL-induced osteoclast differentiation in a dose-dependent manner. TRAP⁺ MNCs having five or more nuclei were considered as osteoclasts. (D, H) TRAP activities were assessed for compounds **1d** and **5d** on osteoclastic activity: *, $p < 0.05$ and **, $p < 0.01$ compared with the RANKL-treated group.

Table 2. IC₅₀ Values of Compounds for RANKL-Induced Osteoclastogenesis from RAW264.7 Cells

compd	IC ₅₀ (μM) ^a	
	TRAP ⁺ MNCs	TRAP activity
1a	10.0 ± 0.7	12.5 ± 1.3
1d	7.1 ± 0.5	10.6 ± 0.7
5d	4.9 ± 0.5	7.3 ± 0.4

^aIC₅₀ is the concentration of tested compound required to inhibit TRAP⁺ MNCs or TRAP activity by 50% of the mean.

activation of mature osteoclasts.^{43,44} The accumulated evidence has suggested that NF-κB is an upstream transcription factor regulating NFATc1 expression.^{12,45} NFATc1 is a key transcription factor involved in osteoclastogenesis and osteoclast formation.^{46,47} Therefore, to investigate the molecular mechanism of **1d**- and **5d**-mediated inhibition of osteoclast differentiation and activation, we performed Western blots to examine NF-κB and NFATc1 in nuclear extracts from RANKL-

activated RAW264.7 cells. As shown in Figure 4, NF-κB and NFATc1 in nuclear extracts were increased after 24 h of treatment with RANKL compared with the levels in RAW264.7 cells without RANKL treatment. Data are expressed as the ratio of the protein level of NF-κB or NFATc1 normalized to TATA-box binding protein (TBP). The elevated levels of nuclear NF-κB and NFATc1 were reduced by **1d** and **5d** in a dose-dependent manner. These results suggest that compounds **1d** and **5d** may suppress RANKL-induced NF-κB and NFATc1 activation during osteoclastogenesis from macrophages.

Effects of **1d and **5d** on RANKL-Induced Bone Resorption in RAW264.7 Cells.** To examine the effects of compounds **1d** and **5d** on osteoclastic bone resorption, we used a pit formation assay to investigate the function of osteoclasts. As shown in Figure 5, resorption pits were formed on the bone slice by osteoclasts after stimulation with RANKL. A dose-dependent attenuation of resorbed areas in the examined slices was observed after treatment with various concentrations of compounds **1d** and **5d**. Furthermore, compounds **1d** and **5d** significantly decreased the percentage of resorbed area relative to the total area at concentrations of 2.5, 5, 7.5, and 10 μM. These results indicate that both compounds prevent osteoclastic bone resorption by inhibiting osteoclastogenesis.

Compounds **1a, **1d**, and **5d** Did Not Affect Osteoblastic Differentiation of MC3T3-E1 Osteoprogenitor Cells.** We investigated the effects of compounds **1a**, **1d**, and **5d** on osteoblastic differentiation using the MC3T3-E1 cell line. As shown in Figure 6, differentiated osteoblasts exhibited ALP activity and ECM deposition in the presence of β-glycerol phosphate and ascorbic acid for 14 days. Compounds **1a**, **1d**, and **5d** did not affect the ALP activity and ECM deposition from MC3T3-E1 cells at a concentration of 7.5 μM. These results indicate that compounds **1a**, **1d**, and **5d** may not impair osteogenesis at concentrations higher than that needed to inhibit osteoclast formation.

CONCLUSIONS

In summary, we synthesized series of salicylanilide analogues (series **a**, **b**, and **c**), 3-phenyl-2*H*-benzo[*e*][1,3]oxazine-2,4(3*H*)-dione analogues (series **d**), and *N*-phenylbenzamide analogues (series **e**) and then evaluated their inhibition of RANKL-induced osteoclastogenesis in preosteoclast RAW264.7 cells. We also studied the SARs of these compounds based on the inhibition of RANKL-induced osteoclast formation. The 2-hydroxyl group of salicylanilide could be the key element related to the activity for inhibition of RANKL-induced osteoclastogenesis. The halogen substituent at the 4-position on benzene ring B of the salicylanilide core may play an important role in the inhibition of osteoclastogenesis, in which the inhibition decreased in the order Cl, I > F, biphenyl group. Furthermore, the new heterocyclic ring-fused compounds **1d** and **5d** exhibited more potent inhibition activities than the other compounds. Both **1d** and **5d** suppressed RANKL-induced osteoclast differentiation, TRAP activity, and bone resorption in a dose-dependent manner. Moreover, compounds **1d** and **5d** showed no significant cytotoxic effects on the cell viability of RAW264.7 cells at 10 μM. Our mechanistic experiments indicated that **1d** and **5d** can inhibit the expression of *NFATc1* and *c-fos* genes as well as osteoclastogenesis-related marker genes (including *DC-STAMP*, *TRAP*, *cathepsin K*, and *MMP-9*) during osteoclastogenesis. The blockade of osteoclastogenesis by **1d** and **5d** might be mediated by attenuation of RANKL-induced NF-κB translocation. We have provided the

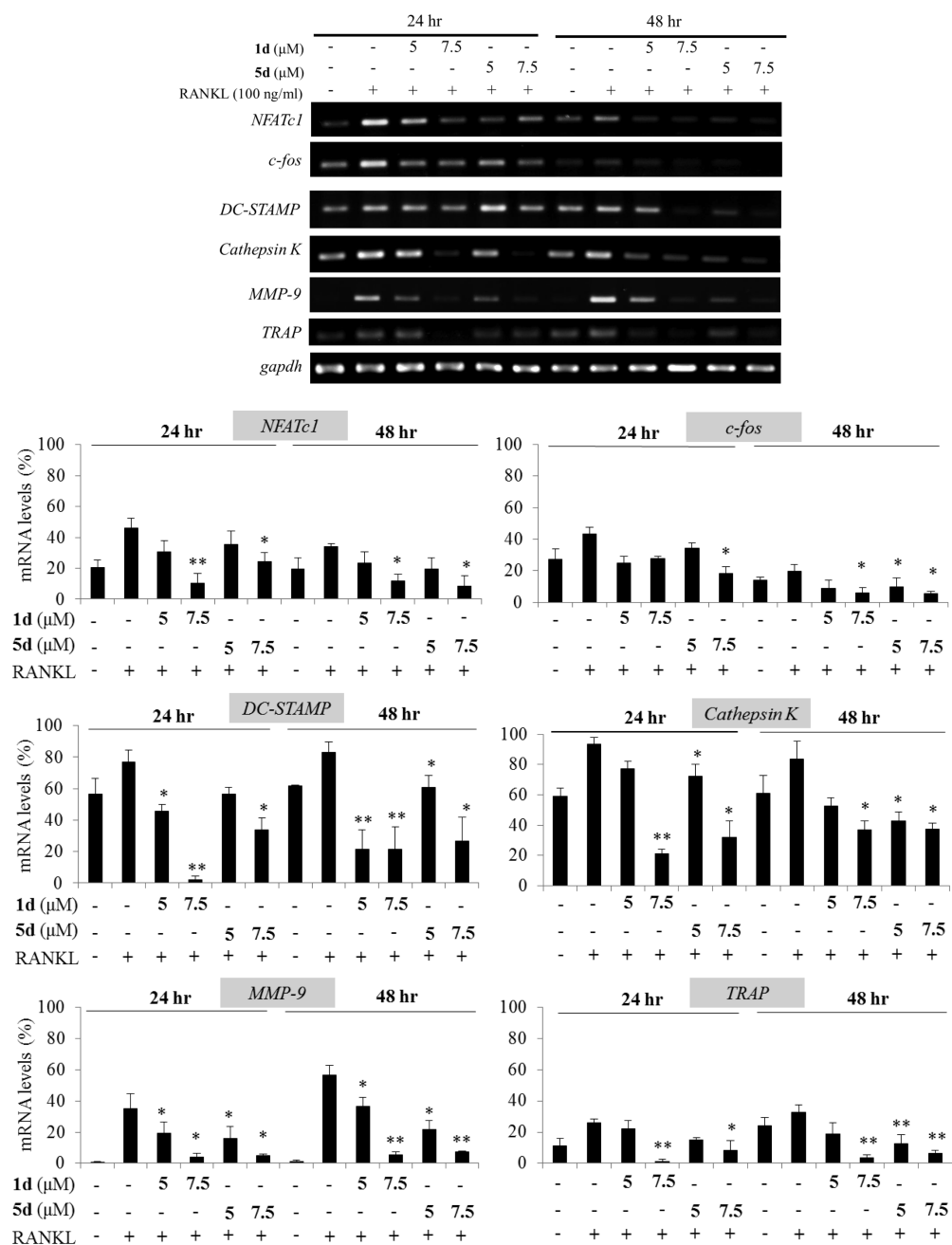


Figure 3. Effects of compounds **1d** and **5d** on osteoclastogenic mRNA expression. RAW264.7 cells were pretreated with or without the tested compounds for 1 h and then supplemented with RANKL (100 ng/mL) for the indicated time points. Total RNA was isolated with TRIzol, and 2 μg of each total RNA was used to transcribe the cDNA. The cDNA was amplified by PCR from mouse-specific primers. Results are expressed as mean \pm SD of three independent experiments. *, $p < 0.05$ and **, $p < 0.01$ compared with the RANKL-treated group.

first evidence that salicylanilides and 3-phenyl-2H-benzo[e][1,3]oxazine-2,4(3H)-dione derivatives inhibit RANKL-induced osteoclastogenesis but do not affect osteogenesis. Therefore, compounds **1d** and **5d** may improve bone health through reducing osteoclast formation and function. Overall, our study indicates that this novel 3-phenyl-2H-benzo[e][1,3]oxazine-2,4(3H)-dione structure offers an attractive starting point for further optimization and represents a promising lead for the development of a new class of antiresorptive agents.

EXPERIMENTAL SECTION

Chemistry. All of the reactions were monitored using TLC plates (silica gel F₂₅₄ plates, Merck). The melting points of compounds were

determined using a Büchi 545 melting point apparatus. ¹H NMR and ¹³C NMR spectra were recorded on an Agilent 400 MR DD2 (400 MHz) apparatus. Mass spectra were obtained using Finnigan MAT-95XL (high-resolution electron impact ionization, HREI) and Finnigan MAT 95S (high-resolution electrospray ionization, HRESI) instruments. The purities of all compounds were analyzed on a C18 reversed-phase column (XBridge BEH Shield RP18 Column, 130 Å, 5 μm , 4.6 mm \times 250 mm, Waters) by HPLC (model I-2000, HITACHI) with UV detection (model I-2400, HITACHI); each compound was dissolved in MeOH, and the mobile phase was water and MeOH. A preliminary evaluation of the UV spectra was carried out by spectrophotometric analysis to determine the value of λ_{max} for each compound. The purities of the synthetic compounds for biological evaluation were greater than 95%. Reagents and solvents were

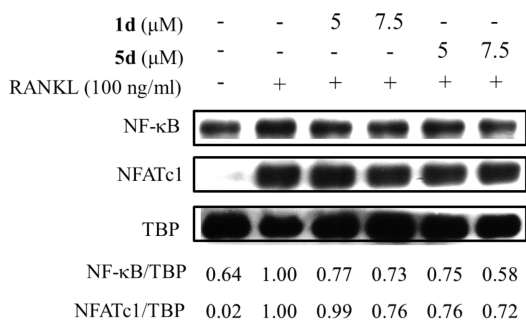


Figure 4. Effects of compounds **1d** and **5d** on RANKL-induced NF-κB and NFATc1 in nuclear extracts. RAW264.7 cells were pretreated with different concentrations of **1d** and **5d** for 1 h prior to treatment with RANKL (100 ng/mL) for 24 h. Nuclear extracts were analyzed by Western blot using antibodies against NF-κB and NFATc1. TBP was evaluated as an internal control.

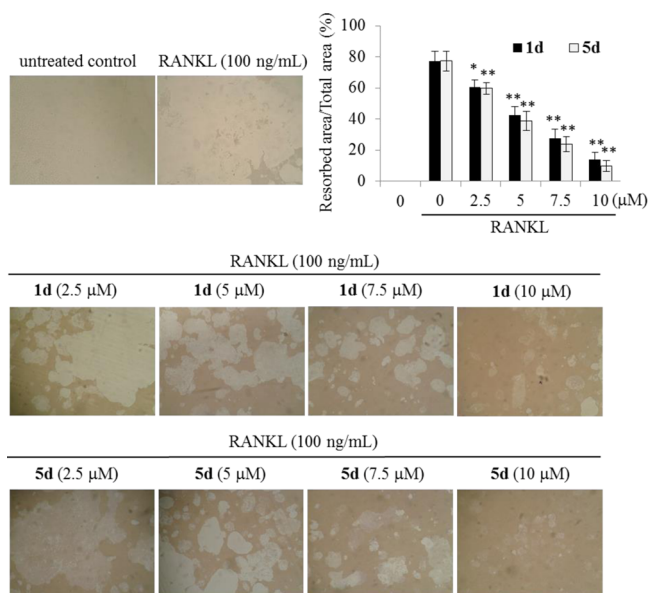


Figure 5. Effects of **1d** and **5d** on resorption pit formation. RAW264.7 cells were cultured on bone slices with various concentrations of compounds **1d** and **5d** in the presence of RANKL (100 ng/mL) for 4 days. After incubation, bone slices were subjected to 0.1% toluidine blue to visualize the resorption pits. Resorbed lacunae on the bone slices were visualized using light microscopy. The ratios of resorbed area relative to the total area were calculated using ImageJ software. *, $p < 0.05$ and **, $p < 0.01$ compared with RANKL-treated group.

purchased from Merck and Sigma-Aldrich and used without further purification.

General Procedure I: Preparation of Compounds 1a–6a. Thionyl chloride (2.5 mL, 34 mmol) was added to a solution of salicylic acid (**1**) (1.38 g, 10 mmol) or 2-hydroxy-4-methoxybenzoic acid (**2**) (1.68 g, 10 mmol) in THF (50 mL) dropwise with stirring. The mixture was refluxed for 3 h and then steam-distilled using a Dean–Stark apparatus, and the produced 2-hydroxybenzoyl chloride or 2-hydroxy-4-methoxybenzoyl chloride was collected. This benzoyl chloride residue was directly refluxed with 4-chloro-2-fluorobenzeneamine (1.1 mL, 10 mmol), 2,4-difluoroaniline (1.0 mL, 10 mmol), or 2-fluoro-4-iodoaniline (2.37 g, 10 mmol) in THF (50 mL) for 12 h. The resulting solution was concentrated and extracted with ethyl acetate. The organic phase was dried over anhydrous magnesium sulfate and concentrated in vacuo. The crude product was crystallized from warm dichloromethane to give the desired compound.

General Procedure II: Preparation of Compounds 1b–6b. Iodomethane (0.28 mL, 4.4 mmol) was added to the mixture of

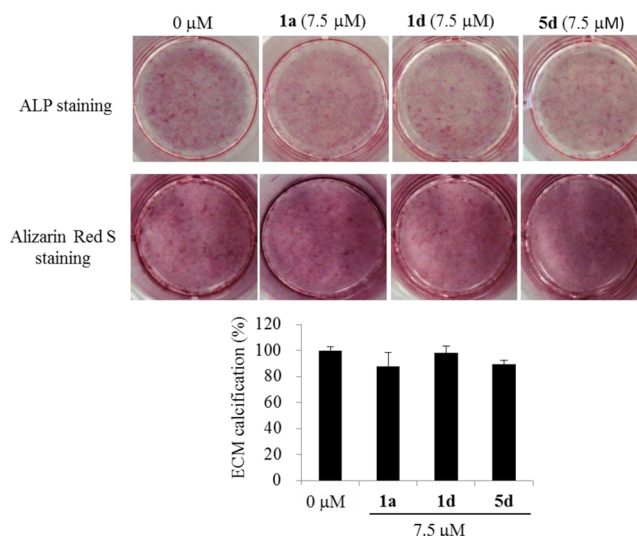


Figure 6. Effects of compounds **1a**, **1d**, and **5d** on osteoblast differentiation from MC3T3-E1 cells. Cells were treated with the tested compounds in the presence of β-glycerol phosphate (10 mM) and ascorbic acid (50 μg/mL) for 14 days, and then the effects of the compounds on ALP activity and ECM calcification were evaluated by the ALP or Alizarin red S staining methods. Furthermore, the ECM calcification was quantified by the amount of cell-bound Alizarin red S. Alizarin red S was released by incubation in 10% cetylpyridinium chloride and then detected by measuring the absorbance at 540 nm. Data are presented as the mean ± SD of three independent experiments.

anhydrous acetone (10 mL), potassium carbonate (0.69 g, 5 mmol), and compound **1a–6a** (2 mmol), and the mixture was refluxed for 8 h. After cooling to room temperature, the reaction mixture was concentrated in vacuo. The residue was extracted with ethyl acetate, dried over anhydrous magnesium sulfate, concentrated, and recrystallized with hot methanol.

General Procedure III: Preparation of Compounds 1c–6c. To a solution of compound **1a–6a** (2 mmol) in anhydrous acetone (10 mL) was added potassium carbonate (0.69 g, 5 mmol) and 2,4-difluorobenzyl bromide (0.56 mL, 4.4 mmol), and the mixture was refluxed for 6 h. After cooling to room temperature, the reaction mixture was concentrated in vacuo. The residue was extracted with ethyl acetate, dried over anhydrous magnesium sulfate, concentrated, and recrystallized with hot methanol.

General Procedure IV: Preparation of Compounds 1d–6d. Methyl chloroformate (0.3 mL, 3.6 mmol) was added dropwise to a stirred solution of **1a–6a** (1 mmol) in dry pyridine (8 mL) at 0 °C, and then the mixture was refluxed for 2 h. After 16 h of stirring at room temperature, the pH of the reaction mixture was adjusted to 6 with 1 N HCl(aq). The resulting white mixture was cooled in an ice bath to obtain a solid compound. The product was filtered and recrystallized from hot ethanol.

General Procedure V: Preparation of Compounds 7a–12a. A mixture of potassium carbonate (1.04 g, 7.5 mmol), palladium(II) acetate (0.034 g, 0.15 mmol), triphenylphosphine (0.131 g, 0.5 mmol), and boronic acid (2,4-difluorophenylboronic acid, 4-chloro-2-fluorophenylboronic acid, or 2,4-dichlorophenylboronic acid) (3.5 mmol) in toluene (20 mL) was added dropwise with constant stirring to a solution of compound **5a** (0.89 g, 2.5 mmol) or **6a** (0.97 g, 2.5 mmol) in toluene (10 mL). The reaction mixture was refluxed for 24 h. After cooling to room temperature, the solution was filtered through Celite and concentrated in vacuo. The crude product was purified using a flash chromatography column with hexane and dichloromethane to give the desired compound as a white solid.

General Procedure VI: Preparation of Compounds 1e–6e. To a solution of aniline (4-chloro-2-fluoroaniline, 2,4-difluoroaniline, or 2-fluoro-4-iodoaniline) (10 mmol) in tetrahydrofuran (40 mL) was

added benzoyl chloride (**3**) (1.16 mL, 10 mmol) or 4-methoxybenzoyl chloride (**4**) (1.35 mL, 10 mmol) with a basic catalyst (TEA, 1.5 mL). The reaction mixture was refluxed for 16 h, concentrated in vacuo, and washed with methanol. The desired product was recrystallized from hot dichloromethane.

N-(4-Chloro-2-fluorophenyl)-2-hydroxybenzamide (1a).²⁵ The pure compound was obtained as a white powder (yield 46%). Mp 187–188 °C. ¹H NMR (400 MHz, CDCl₃): δ 6.95 (t, *J* = 7.6 Hz, 1H), 7.05 (d, *J* = 8.4 Hz, 1H), 7.19–7.22 (m, 2H), 7.48 (t, *J* = 7.8 Hz, 1H), 7.52 (d, *J* = 8.0 Hz, 1H), 8.14 (br, 1H), 8.30 (t, *J* = 8.8 Hz, 1H), 11.67 (s, 1H). ¹³C NMR (100 MHz, CDCl₃): δ 114.17, 115.81, 116.03, 119.06, 119.24, 123.07, 123.08, 124.15, 124.25, 124.97, 125.00, 125.50, 129.86, 129.96, 135.18, 151.46, 153.92, 161.83, 168.12. HRMS (EI) *m/z*: calcd for C₁₃H₉ClFNO₂⁺ [M + H]⁺ 265.0306, found 265.0305.

N-(4-Chloro-2-fluorophenyl)-2-methoxybenzamide (1b). The pure compound was obtained as a white powder (yield 81%). Mp 114–115 °C. ¹H NMR (400 MHz, CDCl₃): δ 4.07 (s, 3H), 7.04 (d, *J* = 8.4 Hz, 1H), 7.12–7.16 (m, 3H), 7.49–7.54 (m, 1H), 8.28 (dd, *J* = 8.0 Hz, *J* = 1.6 Hz, 1H), 8.58 (t, *J* = 9.0 Hz, 1H), 10.34 (s, 1H). ¹³C NMR (100 MHz, CDCl₃): δ 56.20, 111.56, 115.25, 115.48, 121.09, 121.66, 122.32, 122.34, 124.75, 124.79, 126.07, 126.17, 128.04, 128.14, 132.47, 133.67, 150.98, 153.44, 157.35, 163.14. HRMS (EI) *m/z*: calcd for C₁₄H₁₁ClFNO₂⁺ [M + H]⁺ 279.0462, found 279.0458.

N-(4-Chloro-2-fluorophenyl)-2-((2,4-difluorobenzyl)oxy)benzamide (1c). The pure compound was obtained as a white powder (yield 51%). Mp 125–126 °C. ¹H NMR (400 MHz, CDCl₃): δ 5.28 (s, 2H), 6.87–6.95 (m, 2H), 7.02 (dd, *J* = 10.8 Hz, *J* = 2.4 Hz, 1H), 7.10–7.19 (m, 3H), 7.42–7.56 (m, 2H), 8.30 (dd, *J* = 7.6 Hz, *J* = 1.6 Hz, 1H), 8.53 (t, *J* = 8.8 Hz, 1H), 10.04 (s, 1H). ¹³C NMR (100 MHz, CDCl₃): δ 64.92, 64.96, 104.08, 104.33, 104.58, 111.69, 111.73, 111.91, 111.94, 112.68, 115.21, 115.44, 118.05, 118.09, 118.20, 118.23, 121.58, 122.15, 122.45, 122.47, 124.62, 124.66, 125.78, 125.88, 128.15, 128.25, 131.93, 131.97, 132.03, 132.08, 132.78, 133.67, 150.87, 153.33, 156.24, 160.10, 160.22, 162.25, 162.37, 162.60, 162.72, 163.02, 164.75, 164.87. HRMS (ESI) *m/z*: calcd for C₂₀H₁₄ClF₃NO₂⁺ [M + H]⁺ 392.0665, found 392.0673.

3-(4-Chloro-2-fluorophenyl)-2H-benzo[e][1,3]oxazine-2,4(3H)-dione (1d). The pure compound was obtained as a white powder (yield 52%). Mp 180–181 °C. ¹H NMR (400 MHz, CDCl₃): δ 7.30–7.32 (m, 3H), 7.37 (d, *J* = 8.4 Hz, 1H), 7.43 (t, *J* = 7.6 Hz, 1H), 7.78 (t, *J* = 7.8 Hz, 1H), 8.13 (d, *J* = 7.6 Hz, 1H). ¹³C NMR (100 MHz, CDCl₃): δ 113.79, 116.73, 117.54, 117.77, 120.46, 120.60, 125.33, 125.36, 125.84, 128.50, 130.74, 136.51, 136.61, 136.84, 146.89, 152.74, 156.37, 158.91, 159.74. HRMS (ESI) *m/z*: calcd for C₁₄H₈ClFNO₃⁺ [M + H]⁺ 292.0177, found 292.0181.

N-(4-Chloro-2-fluorophenyl)benzamide (1e). The pure compound was obtained as a white powder (yield 95%). Mp 129–130 °C. ¹H NMR (400 MHz, CDCl₃): δ 7.15–7.19 (m, 2H), 7.51 (d, *J* = 7.4 Hz, 2H), 7.57–7.60 (m, 1H), 7.88 (d, *J* = 7.6 Hz, 2H), 8.03 (s, 1H), 8.44 (t, *J* = 8.6 Hz, 1H). ¹³C NMR (100 MHz, CDCl₃): δ 115.53, 115.76, 122.40, 122.41, 124.88, 124.92, 125.25, 125.35, 127.05, 128.92, 129.01, 132.32, 134.13, 151.06, 153.52, 165.37. HRMS (ESI) *m/z*: calcd for C₁₃H₁₀ClFNO⁺ [M + H]⁺ 250.0435, found 250.0431.

N-(4-Chloro-2-fluorophenyl)-2-hydroxy-4-methoxybenzamide (2a). The pure compound was obtained as a white powder (yield 41%). Mp 189–190 °C. ¹H NMR (400 MHz, CDCl₃): δ 3.84 (s, 3H), 6.48–6.51 (m, 2H), 7.17–7.20 (m, 2H), 7.41 (d, *J* = 9.6 Hz, 1H), 7.93 (br, 1H), 8.27 (t, *J* = 8.8 Hz, 1H), 12.09 (s, 1H). ¹³C NMR (100 MHz, CDCl₃): δ 55.55, 101.79, 106.98, 107.77, 115.73, 115.96, 122.98, 124.37, 124.47, 124.91, 124.95, 126.78, 129.45, 129.55, 151.38, 153.84, 164.35, 165.09, 168.02. HRMS (ESI) *m/z*: calcd for C₁₄H₁₂ClFNO₃⁺ [M + H]⁺ 296.0490, found 296.0491.

N-(4-Chloro-2-fluorophenyl)-2,4-dimethoxybenzamide (2b). The pure compound was obtained as a white powder (yield 83%). Mp 155–156 °C. ¹H NMR (400 MHz, CDCl₃): δ 3.86 (s, 3H), 4.02 (s, 3H), 6.51 (d, *J* = 1.6 Hz, 1H), 6.64 (dd, *J* = 8.8 Hz, *J* = 2.0 Hz, 1H), 7.10–7.14 (m, 2H), 8.22 (d, *J* = 8.8 Hz, 1H), 8.57 (t, *J* = 8.8 Hz, 1H), 10.19 (s, 1H). ¹³C NMR (100 MHz, CDCl₃): δ 55.55, 56.13, 98.59, 105.75, 114.00, 115.14, 115.37, 122.12, 122.14, 124.66, 124.70, 126.25, 126.35, 127.62, 127.72, 134.09, 150.84, 153.30, 158.66, 163.01, 164.04.

HRMS (ESI) *m/z*: calcd for C₁₅H₁₄ClFNO₃⁺ [M + H]⁺ 310.0646, found 310.0655.

N-(4-Chloro-2-fluorophenyl)-2-((2,4-difluorobenzyl)oxy)-4-methoxybenzamide (2c). The pure compound was obtained as a yellow powder (yield 53%). Mp 138–139 °C. ¹H NMR (400 MHz, CDCl₃): δ 3.87 (s, 3H), 5.24 (s, 2H), 6.63–6.69 (m, 2H), 6.88–6.95 (m, 2H), 6.99–7.11 (m, 2H), 7.45 (q, *J* = 7.5 Hz, 1H), 8.25 (d, *J* = 8.8 Hz, 1H), 8.53 (t, *J* = 8.6 Hz, 1H), 9.92 (s, 1H). ¹³C NMR (100 MHz, CDCl₃): δ 55.62, 64.78, 64.82, 99.62, 104.07, 104.33, 104.58, 106.32, 111.74, 111.77, 111.95, 111.99, 114.38, 115.13, 115.36, 117.87, 117.91, 118.02, 118.06, 122.31, 122.33, 124.57, 124.60, 125.98, 126.08, 127.76, 127.86, 132.02, 132.06, 132.11, 132.16, 134.41, 150.76, 153.22, 157.50, 160.10, 160.22, 162.25, 162.37, 162.60, 162.72, 162.92, 163.95, 164.75, 164.87. HRMS (ESI) *m/z*: calcd for C₂₁H₁₆ClF₃NO₃⁺ [M + H]⁺ 422.0771, found 422.0778.

3-(4-Chloro-2-fluorophenyl)-7-methoxy-2H-benzo[e][1,3]oxazine-2,4(3H)-dione (2d). The pure compound was obtained as a white powder (yield 41%). Mp 206–207 °C. ¹H NMR (400 MHz, CDCl₃): δ 3.93 (s, 3H), 6.78 (s, 1H), 6.94 (d, *J* = 8.8 Hz, 1H), 7.29–7.31 (m, 3H), 8.01 (d, *J* = 8.8 Hz, 1H), 8.02 (d, *J* = 8.4 Hz, 1H), 8.20 (d, *J* = 8.4 Hz, 1H), 8.26–8.34 (m, 2H). ¹³C NMR (100 MHz, CDCl₃): δ 56.18, 100.35, 106.58, 113.81, 117.51, 117.74, 120.60, 120.74, 125.28, 125.32, 129.88, 130.87, 136.38, 136.48, 147.21, 154.64, 156.45, 158.99, 159.37, 166.51. HRMS (ESI) *m/z*: calcd for C₁₅H₁₀ClFNO₄⁺ [M + H]⁺ 322.0282, found 322.0295.

N-(4-Chloro-2-fluorophenyl)-4-methoxybenzamide (2e). The pure compound was obtained as a white powder (yield 88%). Mp 158–159 °C. ¹H NMR (400 MHz, CDCl₃): δ 3.87 (s, 3H), 6.97 (d, *J* = 8.8 Hz, 2H), 7.13–7.16 (m, 2H), 7.84 (d, *J* = 8.8 Hz, 2H), 7.96 (s, 1H), 8.40 (d, *J* = 8.8 Hz, 1H), 8.44 (t, *J* = 8.6 Hz, 1H). ¹³C NMR (100 MHz, CDCl₃): δ 55.46, 114.06, 115.45, 115.68, 122.36, 124.81, 124.84, 125.44, 125.54, 126.25, 128.56, 128.66, 128.98, 151.03, 153.48, 162.80, 164.84. HRMS (ESI) *m/z*: calcd for C₁₄H₁₂ClFNO₂⁺ [M + H]⁺ 280.0541, found 280.0534.

N-(2,4-Difluorophenyl)-2-hydroxybenzamide (3a).⁴⁸ The pure compound was obtained as a white powder (yield 56%). Mp 186–187 °C. ¹H NMR (400 MHz, CDCl₃): δ 6.95 (t, *J* = 8.6 Hz, 3H), 7.05 (d, *J* = 8.4 Hz, 1H), 7.48 (t, *J* = 7.8 Hz, 1H), 7.53 (d, *J* = 8.0 Hz, 1H), 8.06 (s, 1H), 8.22–8.25 (m, 1H), 11.74 (s, 1H). ¹H NMR (400 MHz, DMSO-*d*₆): δ 6.96–7.01 (m, 2H), 7.10–7.14 (m, 1H), 7.35–7.41 (m, 1H), 7.42–7.47 (m, 1H), 8.00 (d, *J* = 7.6 Hz, 1H), 8.08–8.14 (m, 1H), 8.06 (s, 1H), 8.22–8.25 (m, 1H), 10.60 (s, 1H), 11.92 (s, 1H). ¹³C NMR (100 MHz, DMSO-*d*₆): δ 103.87, 104.12, 104.14, 104.38, 111.18, 111.21, 111.39, 111.43, 117.15, 119.52, 122.52, 122.56, 122.64, 122.67, 124.97, 124.99, 125.06, 125.09, 129.97, 133.98, 152.55, 152.68, 155.01, 155.14, 157.28, 157.39, 157.50, 159.71, 159.82, 165.13. HRMS (ESI) *m/z*: calcd for C₁₃H₁₀F₂NO₂⁺ [M + H]⁺ 250.0680, found 250.0660.

N-(2,4-Difluorophenyl)-2-methoxybenzamide (3b). The pure compound was obtained as a white powder (yield 37%). Mp 87–88 °C. ¹H NMR (400 MHz, CDCl₃): δ 4.07 (s, 3H), 6.87–6.92 (m, 2H), 7.05 (d, *J* = 8.4 Hz, 1H), 7.14 (t, *J* = 7.6 Hz, 1H), 7.50–7.54 (m, 1H), 8.29 (dd, *J* = 7.8 Hz, *J* = 1.8 Hz, 1H), 8.53–8.59 (m, 1H), 10.25 (s, 1H). ¹³C NMR (100 MHz, CDCl₃): δ 56.19, 103.07, 103.31, 103.34, 103.57, 110.98, 111.02, 111.20, 111.23, 111.53, 121.15, 121.64, 122.53, 122.56, 122.62, 122.65, 123.57, 123.68, 132.46, 133.58, 151.21, 151.33, 153.66, 153.77, 156.90, 157.01, 157.34, 159.34, 159.46, 163.12. HRMS (ESI) *m/z*: calcd for C₁₄H₁₂F₂NO₂⁺ [M + H]⁺ 264.0836, found 264.0827.

2-((2,4-Difluorobenzyl)oxy)-N-(2,4-difluorophenyl)benzamide (3c). The pure compound was obtained as a white powder (yield 41%). Mp 135–136 °C. ¹H NMR (400 MHz, CDCl₃): δ 5.29 (s, 2H), 6.75–6.80 (m, 1H), 6.84–6.95 (m, 3H), 7.13–7.19 (m, 2H), 7.43–7.54 (m, 2H), 8.30 (dd, *J* = 7.8 Hz, *J* = 1.8 Hz, 1H), 8.48–8.54 (m, 1H), 9.97 (s, 1H). ¹³C NMR (100 MHz, CDCl₃): δ 64.87, 64.90, 103.00, 103.24, 103.27, 103.50, 104.07, 104.33, 104.58, 110.86, 110.90, 111.08, 111.11, 111.69, 111.73, 111.90, 111.94, 112.64, 118.09, 118.12, 118.24, 118.27, 121.64, 122.12, 122.66, 122.68, 122.75, 122.77, 123.24, 123.27, 123.34, 123.38, 131.88, 131.94, 131.98, 132.03, 132.75, 133.56, 151.10, 151.22, 153.56, 153.67, 156.21, 156.91, 157.02, 159.35, 159.47,

160.06, 160.19, 162.21, 162.33, 162.57, 162.69, 162.99, 164.71, 164.83. HRMS (ESI) m/z : calcd for $C_{20}H_{14}F_4NO_2^+$ $[M + H]^+$ 376.0961, found 376.0955.

3-(2,4-Difluorophenyl)-2H-benzo[e][1,3]oxazine-2,4(3H)-dione (3d). The pure compound was obtained as a white powder (yield 35%). Mp 182–183 °C. 1H NMR (400 MHz, $CDCl_3$): δ 7.01–7.06 (m, 2H), 7.32–7.39 (m, 1H), 7.43 (d, $J = 8.4$ Hz, 1H), 7.43 (t, $J = 7.6$ Hz, 1H), 7.76–7.81 (m, 1H), 8.14 (dd, $J = 8.0$ Hz, $J = 1.6$ Hz, 1H). ^{13}C NMR (100 MHz, $CDCl_3$): δ 105.08, 105.32, 105.35, 105.58, 112.08, 112.12, 112.31, 112.35, 113.84, 116.73, 125.84, 128.53, 130.88, 130.90, 130.98, 131.00, 136.82, 147.08, 152.76, 156.81, 156.93, 159.34, 159.47, 159.90, 161.96, 162.07, 164.47, 164.59. HRMS (ESI) m/z : calcd for $C_{14}H_8F_2NO_3^+$ $[M + H]^+$ 276.0472, found 276.0454.

N-(2,4-Difluorophenyl)benzamide (3e). The pure compound was obtained as a white powder (yield 91%). Mp 120–121 °C. 1H NMR (400 MHz, $CDCl_3$): δ 6.88–6.93 (m, 2H), 7.47–7.51 (m, 2H), 7.55–7.59 (m, 1H), 7.87 (d, $J = 7.2$ Hz, 1H), 8.00 (s, 1H), 8.33–8.39 (m, 1H). ^{13}C NMR (100 MHz, $CDCl_3$): δ 103.32, 103.56, 103.59, 103.83, 111.14, 111.18, 111.36, 111.40, 123.01, 123.03, 123.09, 123.12, 127.04, 128.84, 132.17, 151.55, 151.67, 154.00, 154.11, 157.38, 157.49, 159.83, 159.94, 165.49. HRMS (ESI) m/z : calcd for $C_{13}H_{10}F_2NO^+$ $[M + H]^+$ 234.0730, found 234.0727.

N-(2,4-Difluorophenyl)-2-hydroxy-4-methoxybenzamide (4a). The pure compound was obtained as a white powder (yield 30%). Mp 181–182 °C. 1H NMR (400 MHz, $CDCl_3$): δ 3.84 (s, 3H), 6.49–6.51 (m, 2H), 6.93 (t, $J = 8.6$ Hz, 2H), 7.42 (d, $J = 8.8$ Hz, 1H), 7.85 (s, 1H), 8.19–8.25 (m, 1H), 12.14 (s, 1H). ^{13}C NMR (100 MHz, $CDCl_3$): δ 55.54, 101.78, 103.57, 103.81, 103.84, 104.07, 106.98, 107.69, 111.30, 111.34, 111.52, 111.56, 123.66, 123.76, 123.77, 126.76, 151.93, 152.05, 154.39, 154.51, 157.73, 157.85, 160.20, 160.31, 164.31, 165.01, 168.09. HRMS (ESI) m/z : calcd for $C_{14}H_{12}F_2NO_3^+$ $[M + H]^+$ 280.0785, found 280.0777.

N-(2,4-Difluorophenyl)-2,4-dimethoxybenzamide (4b). The pure compound was obtained as a white powder (yield 33%). Mp 144–145 °C. 1H NMR (400 MHz, $CDCl_3$): δ 3.87 (s, 3H), 4.03 (s, 3H), 6.53 (s, 1H), 6.65 (d, $J = 8.8$ Hz, 1H), 6.88–6.91 (m, 2H), 8.24 (d, $J = 8.8$ Hz, 1H), 8.51–8.57 (m, 1H), 10.11 (s, 1H). ^{13}C NMR (100 MHz, $CDCl_3$): δ 55.58, 56.15, 98.66, 102.99, 103.23, 103.26, 103.49, 105.71, 110.90, 110.94, 111.11, 111.15, 114.12, 122.39, 122.42, 122.48, 122.51, 134.10, 151.11, 151.22, 153.55, 153.67, 156.70, 156.82, 158.68, 159.14, 159.26, 163.03, 163.97. HRMS (ESI) m/z : calcd for $C_{15}H_{14}F_2NO_3^+$ $[M + H]^+$ 294.0942, found 294.0938.

2-((2,4-Difluorobenzyl)oxy)-N-(2,4-difluorophenyl)-4-methoxybenzamide (4c). The pure compound was obtained as a white powder (yield 28%). Mp 132–133 °C. 1H NMR (400 MHz, $CDCl_3$): δ 3.88 (s, 3H), 5.25 (s, 2H), 6.63 (s, 1H), 6.68 (d, $J = 8.8$ Hz, 1H), 6.73–6.79 (m, 1H), 6.83–6.95 (m, 3H), 7.46 (q, $J = 7.6$ Hz, 1H), 8.26 (d, $J = 8.8$ Hz, 1H), 8.47–8.53 (m, 1H), 9.84 (s, 1H). ^{13}C NMR (100 MHz, $CDCl_3$): δ 55.62, 64.80, 99.65, 102.93, 103.16, 103.19, 103.43, 104.08, 104.33, 104.58, 106.29, 110.82, 110.84, 111.02, 111.05, 111.74, 111.78, 111.95, 111.99, 114.50, 117.96, 118.00, 118.11, 122.55, 122.57, 122.63, 122.66, 123.46, 123.50, 123.56, 123.60, 131.95, 132.00, 132.06, 132.10, 134.39, 151.01, 151.13, 153.47, 153.58, 156.73, 156.84, 157.49, 159.17, 159.28, 160.07, 160.20, 162.23, 162.35, 162.58, 162.70, 162.90, 163.87, 164.73, 164.85. HRMS (ESI) m/z : calcd for $C_{21}H_{16}F_4NO_3^+$ $[M + H]^+$ 406.1066, found 406.1067.

3-(2,4-Difluorophenyl)-7-methoxy-2H-benzo[e][1,3]oxazine-2,4(3H)-dione (4d). The pure compound was obtained as a white powder (yield 51%). Mp 142–143 °C. 1H NMR (400 MHz, $CDCl_3$): δ 3.93 (s, 3H), 6.78 (s, 1H), 6.94 (d, $J = 8.8$ Hz, 1H), 7.03 (m, 2H), 7.31–7.36 (m, 1H), 8.02 (d, $J = 8.8$ Hz, 1H). ^{13}C NMR (100 MHz, $CDCl_3$): δ 55.16, 100.33, 105.02, 105.25, 105.28, 105.51, 106.63, 112.00, 112.04, 112.23, 112.26, 113.78, 129.87, 130.98, 130.99, 131.08, 147.38, 154.64, 156.87, 156.99, 159.40, 159.50, 161.89, 162.00, 164.40, 164.51, 166.48. HRMS (ESI) m/z : calcd for $C_{15}H_{10}F_2NO_4^+$ $[M + H]^+$ 306.0578, found 306.0560.

N-(2,4-Difluorophenyl)-4-methoxybenzamide (4e). The pure compound was obtained as a white powder (yield 45%). Mp 134–135 °C. 1H NMR (400 MHz, $CDCl_3$): δ 3.88 (s, 3H), 6.88–7.00 (m, 4H), 7.84–7.86 (m, 2H), 8.36–8.42 (m, 1H). ^{13}C NMR (100 MHz,

$CDCl_3$): δ 55.48, 103.28, 103.51, 103.54, 103.77, 111.16, 111.19, 111.37, 111.41, 114.07, 122.77, 122.80, 122.86, 122.89, 122.99, 123.03, 126.40, 128.97, 151.38, 151.50, 153.83, 153.95, 157.18, 157.30, 159.63, 159.75, 162.75, 164.92. HRMS (ESI) m/z : calcd for $C_{14}H_{12}F_2NO_2^+$ $[M + H]^+$ 264.0836, found 264.0826.

N-(2-Fluoro-4-iodophenyl)-2-hydroxybenzamide (5a). The pure compound was obtained as a white powder (yield 67%). Mp 196–197 °C. 1H NMR (400 MHz, $CDCl_3$): δ 6.93–6.97 (m, 1H), 7.04 (d, $J = 8.4$ Hz, 1H), 7.46–7.54 (m, 4H), 8.10–8.15 (m, 2H), 11.66 (s, 1H). ^{13}C NMR (100 MHz, $CDCl_3$): δ 86.62, 86.70, 114.21, 119.07, 119.25, 123.59, 124.12, 124.34, 125.43, 125.50, 133.94, 133.96, 135.20, 151.17, 153.65, 161.84, 168.09. HRMS (ESI) m/z : calcd for $C_{13}H_{10}FINO_2^+$ $[M + H]^+$ 357.9740, found 357.9729.

N-(2-Fluoro-4-iodophenyl)-2-methoxybenzamide (5b). The pure compound was obtained as a white powder (yield 34%). Mp 183–184 °C. 1H NMR (400 MHz, $CDCl_3$): δ 4.07 (s, 3H), 7.04 (d, $J = 8.4$ Hz, 1H), 7.14 (t, $J = 7.6$ Hz, 1H), 7.44–7.54 (m, 3H), 8.27 (dd, $J = 7.8$ Hz, $J = 1.8$ Hz, 1H), 8.40 (d, $J = 8.4$ Hz, 1H), 10.36 (s, 1H). ^{13}C NMR (100 MHz, $CDCl_3$): δ 56.21, 84.64, 84.72, 111.54, 121.06, 121.66, 123.04, 123.05, 123.54, 123.76, 127.28, 127.37, 132.47, 133.72, 133.77, 133.81, 150.81, 153.28, 157.33, 163.16. HRMS (ESI) m/z : calcd for $C_{14}H_{12}FINO_2^+$ $[M + H]^+$ 371.9897, found 371.9906.

2-((2,4-Difluorobenzyl)oxy)-N-(2-fluoro-4-iodophenyl)benzamide (5c). The pure compound was obtained as a white powder (yield 60%). Mp 135–136 °C. 1H NMR (400 MHz, $CDCl_3$): δ 5.28 (s, 2H), 6.87–6.95 (m, 2H), 7.13–7.19 (m, 2H), 7.33 (dd, $J = 10.2$ Hz, $J = 1.8$ Hz, 1H), 7.42–7.48 (m, 2H), 7.50–7.55 (m, 1H), 8.29 (dd, $J = 7.8$ Hz, $J = 1.8$ Hz, 1H), 8.35 (t, $J = 8.4$ Hz, 1H), 10.06 (s, 1H). ^{13}C NMR (100 MHz, $CDCl_3$): δ 64.90, 64.94, 84.80, 84.87, 104.09, 104.34, 104.60, 111.70, 111.74, 111.92, 111.96, 112.64, 117.99, 118.04, 118.14, 118.18, 121.55, 122.15, 123.16, 123.51, 123.73, 127.00, 127.10, 131.96, 132.00, 132.05, 132.10, 132.79, 133.64, 133.68, 133.71, 150.69, 153.17, 156.23, 160.11, 160.23, 162.25, 162.36, 162.61, 162.73, 163.03, 164.74, 164.86. HRMS (ESI) m/z : calcd for $C_{20}H_{12}F_3INO_2^-$ $[M - H]^-$ 481.9865, found 481.9884.

3-(2-Fluoro-4-iodophenyl)-2H-benzo[e][1,3]oxazine-2,4(3H)-dione (5d). The pure compound was obtained as a white powder (yield 41%). Mp 183–184 °C. 1H NMR (400 MHz, $CDCl_3$): δ 7.01–7.11 (m, 1H), 7.37 (dd, $J = 8.2$ Hz, $J = 0.6$ Hz, 1H), 7.41–7.45 (m, 1H), 7.63–7.67 (m, 2H), 7.76–7.81 (m, 1H), 8.14 (dd, $J = 7.8$ Hz, $J = 1.4$ Hz, 1H). ^{13}C NMR (100 MHz, $CDCl_3$): δ 95.01, 95.09, 113.81, 116.75, 125.87, 126.17, 126.39, 128.54, 131.28, 134.29, 134.33, 136.86, 152.76, 156.07, 158.63, 159.67. HRMS (ESI) m/z : calcd for $C_{14}H_8FINO_3^+$ $[M + H]^+$ 383.9533, found 383.9558.

N-(2-Fluoro-4-iodophenyl)benzamide (5e). The pure compound was obtained as a white powder (yield 61%). Mp 153–154 °C. 1H NMR (400 MHz, $CDCl_3$): δ 7.47–7.53 (m, 4H), 7.57–7.61 (m, 1H), 7.88 (d, $J = 8.0$ Hz, 2H), 8.02 (s, 1H), 8.27 (t, $J = 8.4$ Hz, 1H). ^{13}C NMR (100 MHz, $CDCl_3$): δ 85.57, 85.65, 123.01, 123.02, 123.83, 124.05, 127.05, 128.92, 132.33, 133.85, 133.89, 134.13, 150.83, 153.30, 165.32. HRMS (ESI) m/z : calcd for $C_{13}H_{10}FINO^+$ $[M + H]^+$ 341.9791, found 341.9798.

N-(2-Fluoro-4-iodophenyl)-2-hydroxy-4-methoxybenzamide (6a). The pure compound was obtained as a white powder (yield 40%). Mp 214–215 °C. 1H NMR (400 MHz, $CDCl_3$): δ 3.85 (s, 3H), 6.49–6.51 (m, 2H), 7.41 (d, $J = 8.8$ Hz, 1H), 7.49–7.52 (m, 2H), 7.94 (s, 1H), 8.11 (t, $J = 8.4$ Hz, 1H), 12.08 (s, 1H). ^{13}C NMR (100 MHz, $CDCl_3$): δ 51.59, 86.13, 86.21, 101.80, 107.02, 107.78, 123.50, 124.03, 124.24, 125.65, 125.75, 126.76, 133.87, 133.91, 151.09, 153.57, 164.38, 165.11, 167.98. HRMS (ESI) m/z : calcd for $C_{14}H_{12}FINO_3^+$ $[M + H]^+$ 387.9846, found 387.9862.

N-(2-Fluoro-4-iodophenyl)-2,4-dimethoxybenzamide (6b). The pure compound was obtained as a white powder (yield 30%). Mp 118–119 °C. 1H NMR (400 MHz, $CDCl_3$): δ 3.88 (s, 3H), 4.03 (s, 3H), 6.53 (d, $J = 1.6$ Hz, 1H), 6.65 (dd, $J = 8.8$ Hz, $J = 2.0$ Hz, 1H), 7.43–7.48 (m, 2H), 8.23 (d, $J = 8.8$ Hz, 1H), 8.39 (t, $J = 8.4$ Hz, 1H), 10.22 (s, 1H). ^{13}C NMR (100 MHz, $CDCl_3$): δ 55.60, 56.19, 84.22, 84.30, 98.67, 105.79, 114.10, 122.95, 122.97, 123.46, 123.67, 127.50, 127.60, 133.73, 133.77, 134.18, 150.75, 153.23, 158.71, 163.06, 164.10.

HRMS (ESI) m/z : calcd for $C_{15}H_{14}FINO_3^+$ $[M + H]^+$ 402.0002, found 402.0014.

2-((2,4-Difluorobenzyl)oxy)-N-(2-fluoro-4-iodophenyl)-4-methoxybenzamide (6c). The pure compound was obtained as a white powder (yield 27%). Mp 152–153 °C. 1H NMR (400 MHz, $CDCl_3$): δ 3.87 (s, 3H), 5.24 (s, 2H), 6.63–6.68 (m, 2H), 6.87–6.95 (m, 2H), 7.30–7.32 (m, 1H), 7.41–7.46 (m, 2H), 8.24 (d, $J = 8.8$ Hz, 1H), 8.35 (t, $J = 8.4$ Hz, 1H), 9.93 (s, 1H). ^{13}C NMR (100 MHz, $CDCl_3$): δ 55.62, 64.79, 64.82, 84.35, 84.43, 99.61, 104.07, 104.32, 104.58, 106.33, 111.73, 111.77, 111.95, 111.98, 114.40, 117.85, 117.89, 118.00, 118.03, 123.06, 123.41, 123.63, 127.22, 127.32, 132.03, 132.08, 132.13, 132.18, 133.57, 133.61, 134.42, 150.62, 153.10, 157.50, 160.10, 160.23, 162.25, 162.37, 162.61, 162.73, 162.92, 163.98, 164.75, 164.87. HRMS (ESI) m/z : calcd for $C_{21}H_{16}F_3INO_3^+$ $[M + H]^+$ 514.0127, found 514.0139.

3-(2-Fluoro-4-iodophenyl)-7-methoxy-2H-benzo[e][1,3]oxazine-2,4(3H)-dione (6d). The pure compound was obtained as a white powder (yield 69%). Mp 200–201 °C. 1H NMR (400 MHz, $CDCl_3$): δ 6.78 (d, $J = 2.0$ Hz, 1H), 6.94 (dd, $J = 2.0$ Hz, $J = 9.0$ Hz, 1H), 7.06–7.10 (m, 1H), 7.62–7.64 (m, 2H), 8.02 (d, $J = 8.8$ Hz, 1H). ^{13}C NMR (100 MHz, $CDCl_3$): δ 56.16, 94.82, 94.90, 100.34, 106.56, 113.78, 121.88, 122.01, 126.08, 126.30, 129.86, 131.39, 134.20, 134.24, 147.08, 154.62, 156.12, 158.69, 159.25, 166.48. HRMS (ESI) m/z : calcd for $C_{15}H_{10}FINO_4^+$ $[M + H]^+$ 413.9639, found 413.9644.

N-(2-Fluoro-4-iodophenyl)-4-methoxybenzamide (6e). The pure compound was obtained as a white powder (yield 72%). Mp 161–162 °C. 1H NMR (400 MHz, $CDCl_3$): δ 3.87 (s, 3H), 6.98 (d, $J = 8.8$ Hz, 2H), 7.44–7.49 (m, 2H), 7.83 (d, $J = 8.8$ Hz, 2H), 7.96 (s, 1H), 8.24 (t, $J = 8.4$ Hz, 1H). ^{13}C NMR (100 MHz, $CDCl_3$): δ 55.48, 85.18, 85.26, 114.08, 122.97, 122.98, 123.75, 123.97, 129.00, 133.80, 133.84, 150.81, 153.28, 162.82, 164.81. HRMS (ESI) m/z : calcd for $C_{14}H_{12}FINO_2^+$ $[M + H]^+$ 371.9897, found 371.9921.

2-Hydroxy-N-(2',3,4'-trifluoro-[1,1'-biphenyl]-4-yl)benzamide (7a). The pure compound was obtained as a white powder (yield 52%). Mp 194–195 °C. 1H NMR (400 MHz, $CDCl_3$): δ 6.90–6.99 (m, 3H), 7.06 (d, $J = 8.4$ Hz, 1H), 7.33–7.44 (m, 3H), 7.46–7.50 (m, 1H), 7.56 (d, $J = 8.0$ Hz, 1H), 8.24 (s, 1H), 8.42 (t, $J = 8.6$ Hz, 1H), 11.79 (s, 1H). ^{13}C NMR (100 MHz, $CDCl_3$): δ 104.34, 104.59, 104.85, 111.71, 111.74, 111.92, 111.96, 114.33, 115.44, 115.47, 115.64, 115.68, 119.05, 119.21, 122.23, 124.82, 124.92, 125.04, 125.07, 125.10, 125.53, 131.06, 131.11, 131.15, 131.20, 132.11, 132.20, 135.11, 151.50, 153.92, 158.38, 158.50, 160.88, 161.00, 161.23, 161.34, 161.90, 163.72, 163.83, 168.21. HRMS (ESI) m/z : calcd for $C_{19}H_{13}F_3NO_2^+$ $[M + H]^+$ 344.0898, found 344.0905.

2-Hydroxy-4-methoxy-N-(2',3,4'-trifluoro-[1,1'-biphenyl]-4-yl)benzamide (8a). The pure compound was obtained as a white powder (yield 17%). Mp 211–212 °C. 1H NMR (400 MHz, $CDCl_3$): δ 3.85 (s, 3H), 6.51–6.53 (m, 2H), 6.90–6.99 (m, 2H), 7.32–7.47 (m, 4H), 8.04 (s, 1H), 8.40 (t, $J = 8.2$ Hz, 1H), 12.19 (s, 1H). ^{13}C NMR (100 MHz, $CDCl_3$): δ 55.55, 101.83, 104.32, 104.59, 104.84, 107.19, 107.72, 111.69, 111.72, 111.90, 111.93, 115.38, 115.42, 115.59, 115.63, 122.17, 125.04, 125.07, 125.17, 126.82, 131.06, 131.11, 131.15, 131.20, 131.75, 131.83, 151.44, 153.86, 158.39, 158.51, 160.89, 161.01, 161.20, 161.32, 163.69, 163.80, 164.40, 165.07, 168.12. HRMS (ESI) m/z : calcd for $C_{20}H_{13}F_3NO_3^+$ $[M + H]^+$ 374.1004, found 374.1029.

N-(4'-Chloro-2',3-difluoro-[1,1'-biphenyl]-4-yl)-2-hydroxybenzamide (9a). The pure compound was obtained as a white powder (yield 22%). Mp 206–207 °C. 1H NMR (400 MHz, $CDCl_3$): δ 6.97 (t, $J = 7.6$ Hz, 1H), 7.06 (d, $J = 8.4$ Hz, 1H), 7.20–7.24 (m, 2H), 7.36–7.40 (m, 3H), 7.49 (t, $J = 8.7$ Hz, 1H), 7.56 (d, $J = 8.0$ Hz, 1H), 8.25 (s, 1H), 8.43 (t, $J = 8.6$ Hz, 1H), 11.77 (s, 1H). ^{13}C NMR (100 MHz, $CDCl_3$): δ 114.31, 115.41, 115.43, 115.62, 115.66, 116.93, 117.19, 119.07, 119.22, 122.22, 125.00, 125.03, 125.07, 125.19, 125.52, 125.76, 130.97, 131.01, 131.82, 131.91, 134.41, 134.52, 135.15, 151.46, 153.89, 158.13, 160.64, 161.92, 168.21. HRMS (ESI) m/z : calcd for $C_{19}H_{13}ClF_2NO_2^+$ $[M + H]^+$ 360.0603, found 360.0621.

N-(4'-Chloro-2',3-difluoro-[1,1'-biphenyl]-4-yl)-2-hydroxy-4-methoxybenzamide (10a). The pure compound was obtained as a white powder (yield 27%). Mp 233–234 °C. 1H NMR (400 MHz, $CDCl_3$): δ 3.86 (s, 3H), 6.51–6.53 (m, 2H), 7.19–7.23 (m, 2H), 7.34–7.47 (m,

3H), 8.05 (s, 1H), 8.41 (t, $J = 8.4$ Hz, 1H), 12.16 (s, 1H). ^{13}C NMR (100 MHz, $CDCl_3$): δ 55.56, 101.84, 107.18, 107.75, 107.79, 115.36, 115.56, 115.60, 116.92, 117.18, 122.16, 123.54, 124.05, 124.27, 124.98, 125.01, 125.33, 125.44, 126.78, 126.83, 130.97, 131.02, 133.90, 133.94, 134.34, 134.45, 151.42, 153.84, 158.15, 160.66, 164.42, 165.10, 168.12. HRMS (ESI) m/z : calcd for $C_{20}H_{15}ClF_2NO_3^+$ $[M + H]^+$ 390.0709, found 390.0730.

N-(2',4'-Dichloro-3-fluoro-[1,1'-biphenyl]-4-yl)-2-hydroxybenzamide (11a). The pure compound was obtained as a white powder (yield 18%). Mp 208–209 °C. 1H NMR (400 MHz, $CDCl_3$): δ 6.98 (t, $J = 7.6$ Hz, 1H), 7.08 (d, $J = 8.4$ Hz, 1H), 7.28–7.35 (m, 4H), 7.49–7.52 (m, 2H), 7.58 (d, $J = 8.0$ Hz, 1H), 8.26 (s, 1H), 8.43 (t, $J = 8.2$ Hz, 1H), 11.79 (s, 1H). ^{13}C NMR (100 MHz, $CDCl_3$): δ 114.32, 116.09, 116.29, 119.08, 119.23, 121.95, 125.05, 125.15, 125.52, 125.79, 125.82, 127.36, 129.92, 131.91, 133.15, 134.28, 135.14, 135.36, 135.44, 137.14, 151.13, 153.56, 161.92, 168.24. HRMS (ESI) m/z : calcd for $C_{19}H_{13}Cl_2FNO_2^+$ $[M + H]^+$ 376.0307, found 376.0318.

N-(2',4'-Dichloro-3-fluoro-[1,1'-biphenyl]-4-yl)-2-hydroxy-4-methoxybenzamide (12a). The pure compound was obtained as a white powder (yield 60%). Mp 223–224 °C. 1H NMR (400 MHz, $CDCl_3$): δ 3.88 (s, 3H), 6.54–6.56 (m, 2H), 7.28–7.36 (m, 4H), 7.48–7.50 (m, 1H), 7.54 (d, $J = 2.0$ Hz, 1H), 8.09 (s, 1H), 8.43 (t, $J = 2.0$ Hz, 1H), 12.21 (s, 1H). ^{13}C NMR (100 MHz, $CDCl_3$): δ 55.56, 101.83, 107.17, 107.75, 116.02, 116.22, 121.87, 125.28, 125.38, 125.74, 125.78, 126.83, 127.34, 129.90, 131.92, 133.16, 134.22, 134.98, 135.06, 137.22, 151.07, 153.50, 164.40, 165.08, 168.13. HRMS (ESI) m/z : calcd for $C_{20}H_{15}Cl_2FNO_3^+$ $[M + H]^+$ 406.0413, found 406.0446.

RAW264.7 Cell Culture. The murine monocyte/macrophage cell line RAW264.7 (purchased from ATCC, USA) was cultured in DMEM (Gibco BRL) containing 10% heat-inactivated FBS. The cells were grown at 37 °C in a humid atmosphere containing 5% CO_2 .

Cell Viability by MTT Assay. The tetrazolium reagent 3-(4,5-dimethylthiazol-2-yl)-2,5-diphenyltetrazolium bromide (MTT) was designed to yield a formazan product upon metabolic reduction by viable cells.⁴⁹ RAW264.7 cells (1×10^4 cells/well) were seeded in 96-well plates with DMEM supplemented with 10% FBS and treated with various concentrations of synthetic compounds for 24 h. After compound treatment, the 96-well plates were washed with PBS three times, and then MTT solution (100 μ L, 0.5 mg/mL) in the medium was added to each well for 1 h at 37 °C. The cells were then washed with PBS and solubilized in 100 μ L of DMSO per well. The absorbances at 540 nm were determined with an ELISA microplate reader. The effects of compounds on cell viability were shown as relative activity (% of compound-treated group relative to the DMSO control group).

RANKL-Induced Osteoclast Differentiation and Measurements of TRAP Activity. RAW264.7 cells were seeded at a density of 1×10^3 cells/well in 96-well plates or 5×10^4 cells/well in 48-well plates and cultured in α -MEM (Gibco BRL) containing 10% FBS, 2 mM L-glutamate, 100 ng/mL recombinant soluble murine RANKL (Peprotec), and various concentrations of synthetic compounds for 4 days. Cell culture media were changed on day 2. For RANKL-induced osteoclast differentiation, cells were fixed with the fixing solution (65:25:8 acetone/citrate solution/37% formaldehyde) for 5 min. Multinucleated osteoclasts were quantified by determining cells that were TRAP-positive [stained by tartrate-resistant acid phosphatase kit (Sigma-Aldrich, 387A-1KT)]. The red TRAP-positive multinucleated cells (>5 nuclei/cell) were visualized by light microscopy and counted as mature osteoclasts. The effects of compounds on RANKL-induced osteoclast differentiation were shown as the percentage of TRAP-positive multinucleated cells (% of the compound-treated group relative to the RANKL-treated group).

For measurement of the TRAP activity, the cells were washed with PBS on day 4, and 100 μ L of lysis solution (0.1% Triton X-100 in 50 mM Tris-HCl, pH 7.2) was added to each well for 15 min on ice. Subsequently, 100 μ L of the substrate solution (2 mg/mL 4-nitrophenyl phosphate in 0.09 M citrate buffer, Sigma-Aldrich) was added to each well, and the wells were incubated for 15 min at 37 °C. To stop the reaction, the reaction mixtures in the wells were transferred to new plates containing NaOH(aq) (200 μ L, 0.1 N).

Table 3. Primers Used for RT-PCR

target gene	forward primer sequence (5'–3')	reverse primer sequence (5'–3')
<i>NFATc1</i>	CCCTGACCACCGATAGCACTCT	GGTGCCTTCCGCTCATAGTG
<i>c-fos</i>	GGTTTCAACGCCGACTACGAG	CTGACACGGTCTTACCATTCC
<i>DC-STAMP</i>	CCGCTGTGGACTATCTGCTGTA	TTCCCGTCAGCCTCTCTCAAT
<i>cathepsin K</i>	AGGCAGCTAAATGCAGAGGGTA	CAGGCGTTGTTCTTATTCCGAG
<i>MMP-9</i>	AGGCCTCTACAGAGTCTTTG	CAGTCCAACAGAAAGGACG
<i>TRAP</i>	ACGGCTACTTGCGGTTTCACTA	GTGTGGGCATACTTCTTTCCTGT
<i>GAPDH</i>	GTGAGGCCGGTGCTGAGTATGT	ACAGTCTTCTGGGTGGCAGTGAT

Absorbances were measured at 405 nm with the ELISA reader. The effects of compounds on RANKL-induced TRAP activity from osteoclasts were shown as relative activity (% of the compound-treated group relative to the RANKL-treated group).

RT-PCR Analysis. RAW264.7 cells were suspended in DMEM containing 10% FBS and seeded onto 6 cm dishes at a density of 1×10^5 cells/plate. After 1 day, cells were starved for 24 h by replacing the DMEM with α -MEM and subsequently exposed to 100 ng/mL RANKL and various concentrations of the tested compounds for either 24 or 48 h. Total RNA was isolated from the cultured cells with TRIzol reagent (Invitrogen). The RNA (2 μ g each) was reversibly transcribed using SuperScript II reverse transcriptase (Invitrogen) and oligo-(dT)₁₅ primer. The cDNA was amplified using mouse-specific primer (Table 3). Each of the PCR experiments was performed in 25 μ L of 10 mM Tris-HCl (pH 8.8), 1.5 mM MgCl₂, 50 mM KCl, 0.1% Triton X-100, 1 unit of DNA polymerase (Protech), 200 μ M dNTP, and 10 μ M primer. The PCR products were separated on 1.5% agarose gels, and the bands were visualized by ethidium bromide staining. The optical densities for each gene were normalized to the corresponding values for *gapdh* gene.

Western Blot Analysis. RAW264.7 cells were seeded at a density of 1×10^6 cells in 6 cm culture plates containing DMEM with 10% FBS and incubated for 24 h to become attached. Cells were pretreated with different concentrations of compounds in α -MEM containing 10% FBS for 1 h prior to treatment with RANKL (100 ng/mL) for 24 h. The cells were then harvested and washed with cold PBS. Nuclear protein extracts from RAW264.7 cells were prepared using NE-PER nuclear and cytoplasmic extraction reagents (Thermo Fisher Scientific) according to the manufacturer's instructions. Nuclear protein extracts (18 μ g) were electrophoresed on 12% SDS-PAGE gels and transferred to Immobilon poly(vinyl difluoride) members. Nonspecific binding was blocked by soaking the members in TBS buffer containing 5% BSA for 1 h. The blots were probed with anti-NFATc1 (clone 7A6, Santa Cruz Biotechnology), anti-NF- κ B (clone E379, Epitomics), or anti-TATA box-binding protein (clone 1TBP18, Abcam) monoclonal antibodies (1:1000) for 12 h at 4 °C. After further washing with TBST, the blots were subsequently incubated with a secondary antibody coupled to horseradish peroxidase (1:10000) for 1 h. The immunoreactive bands were visualized using the Immobilon Western chemiluminescent HRP substrate kit (Millipore) and exposing a clear blue X-ray film (Thermo Fisher Scientific) to the membrane. The optical densities for each NF- κ B or NFATc1 protein were normalized to the corresponding values for TBP.

Pit Formation Assay. To assess the effects of compounds on RANKL-induced bone resorption, RAW264.7 cells were suspended in α -MEM containing 10% FBS and seeded (1×10^4 cells/well) onto dentine slices (24 well plates, Corning) in the presence or absence of 100 ng/mL RANKL and compounds. The media of all of the cultured cells were replaced every 2 days with fresh media containing the test chemicals. After 4 days of culture, the wells were washed three times with PBS and filled with 1 M ammonium hydroxide to remove the attached cells that were stained with 0.1% toluidine blue (Sigma-Aldrich). The ratios of resorbed area to total area were measured in the optical field of the slice using ImageJ software.

Osteoblast Differentiation of MC3T3-E1 Cells. The mouse calvaria-origin cell line MC3T3-E1 (purchased from ATCC, USA) was maintained in α -MEM (Gibco BRL) with 10% heat-inactivated FBS in

the absence of ascorbic acid. The cells were grown at 37 °C in a humid atmosphere containing 5% CO₂. For the determination of osteoblast differentiation, the cells were seeded at a density of 2.5×10^4 cells/well in a 24-well plate and cultured in α -MEM containing 10% FBS, 2 mM L-glutamate, 10 mM β -glycerol phosphate (Sigma-Aldrich), 50 μ g/mL ascorbic acid (Sigma-Aldrich), and various concentrations of the tested compounds for 14 days. Cell culture media were changed every 3 days. After 14 days, ECM calcification and ALP staining of the osteoblastic MC3T3-E1 cells were measured as described in the next section.

ALP Staining and Measurement of ECM Calcification. ALP staining of the osteoblastic MC3T3-E1 cells was performed using the ALP staining kit (Sigma-Aldrich 86R-1KT). After osteoblast differentiation, cells were fixed with the fixing solution (65:25:8 acetone/citrate solution/37% formaldehyde) for 10 min. The ALP staining of cells was assayed using the enzymatic kit according to the manufacturer's instructions. The stained cells were washed extensively with distilled water and imaged using a camera.

The Alizarin red S staining method was used to determine the ECM calcification of osteoblasts in vitro. After culture protocol as described above, cells were fixed with 4% paraformaldehyde for 30 min and stained with 2% Alizarin red S (Sigma-Aldrich). Alizarin red S staining for calcium precipitation was imaged using a camera. To quantify the ECM calcium deposits in the cell matrix, the staining of cells was eluted with 100 μ L of 10% cetylpyridinium chloride and quantified by measuring the absorbance at 540 nm. The absorbance was shown as relative activity (% of the compound-treated group relative to the DMSO control group).

■ ASSOCIATED CONTENT

📄 Supporting Information

Inhibitory effects of **1a** against RANKL-induced osteoclast differentiation and NMR spectra of compounds **1a**, **1d**, **5a**, and **5d**. This material is available free of charge via the Internet at <http://pubs.acs.org>.

■ AUTHOR INFORMATION

Corresponding Authors

*D.M.C: Tel: 886-2-28757799. Fax: +886-2-77351333. E-mail: ming0503@ms3.hinet.net.

*H.S.H: Tel: 886-2-27361661 ext 7525. Fax: 886-2-66387537. E-mail: huanghs99@tmu.edu.tw.

Notes

The authors declare no competing financial interest.

■ ACKNOWLEDGMENTS

We thank Orient Europharma Co. Ltd., Taiwan, for their assistance in supporting our research. The present study was also supported by the National Science Council (Grants 101-2113-M-016-001 and 102-2314-B-016-059-MY3) and the Chi-Mei Medical Center (Grant CMNDMC-10210).

■ ABBREVIATIONS USED

RA, rheumatoid arthritis; RANKL, receptor activator of nuclear factor- κ B ligand; TNF, tumor necrosis factor; NFATc1, nuclear

factor of activated T cells c1; TRAP, tartrate-resistant acid phosphatase; SAR, structure–activity relationship; DC-STAMP, dendritic cell-specific transmembrane protein; MMP, matrix metalloproteinase; ALP, alkaline phosphatase; HRMS, high-resolution mass spectrometry; TBP, TATA-box binding protein; ECM, extracellular matrix; DMSO, dimethyl sulfoxide; THF, tetrahydrofuran; TEA, triethylamine.

REFERENCES

- (1) Goltzman, D. Discoveries, drugs and skeletal disorders. *Nat. Rev. Drug Discovery* **2002**, *1*, 784–796.
- (2) Boyle, W. J.; Simonet, W. S.; Lacey, D. L. Osteoclast differentiation and activation. *Nature* **2003**, *423*, 337–342.
- (3) Romas, E.; Gillespie, M. T.; Martin, T. J. Involvement of receptor activator of NF κ B ligand and tumor necrosis factor- α in bone destruction in rheumatoid arthritis. *Bone* **2002**, *30*, 340–246.
- (4) Tanaka, S. Signaling axis in osteoclast biology and therapeutic targeting in the RANKL/RANK/OPG system. *Am. J. Nephrol.* **2007**, *27*, 466–478.
- (5) Walsh, N. C.; Gravallesse, E. M. Bone loss in inflammatory arthritis: Mechanisms and treatment strategies. *Curr. Opin. Rheumatol.* **2004**, *16*, 419–427.
- (6) Kearns, A. E.; Khosla, S.; Kostenuik, P. J. Receptor activator of nuclear factor κ B ligand and osteoprotegerin regulation of bone remodeling in health and disease. *Endocr. Rev.* **2008**, *29*, 155–192.
- (7) Teitelbaum, S. L. Bone resorption by osteoclasts. *Science* **2000**, *289*, 1504–1508.
- (8) Suda, T.; Takahashi, N.; Udagawa, N.; Jimi, E.; Gillespie, M. T.; Martin, T. J. Modulation of osteoclast differentiation and function by the new members of the tumor necrosis factor receptor and ligand families. *Endocr. Rev.* **1999**, *20*, 345–357.
- (9) Darnay, B. G.; Haridas, V.; Ni, J.; Moore, P. A.; Aggarwal, B. B. Characterization of the intracellular domain of receptor activator of NF- κ B (RANK). Interaction with tumor necrosis factor receptor-associated factors and activation of NF- κ B and c-Jun N-terminal kinase. *J. Biol. Chem.* **1998**, *273*, 20551–20555.
- (10) Kikuta, J.; Ishii, M. Osteoclast migration, differentiation and function: Novel therapeutic targets for rheumatic diseases. *Rheumatology (Oxford, U. K.)* **2013**, *52*, 226–234.
- (11) Koga, T.; Matsui, Y.; Asagiri, M.; Kodama, T.; de Crombrughe, B.; Nakashima, K.; Takayanagi, H. NFAT and Osterix cooperatively regulate bone formation. *Nat. Med.* **2005**, *11*, 880–885.
- (12) Takayanagi, H.; Kim, S.; Koga, T.; Nishina, H.; Isshiki, M.; Yoshida, H.; Saiura, A.; Isobe, M.; Yokochi, T.; Inoue, J.; Wagner, E. F.; Mak, T. W.; Kodama, T.; Taniguchi, T. Induction and activation of the transcription factor NFATc1 (NFAT2) integrate RANKL signaling in terminal differentiation of osteoclasts. *Dev. Cell* **2002**, *3*, 889–901.
- (13) Kim, Y.; Sato, K.; Asagiri, M.; Morita, I.; Soma, K.; Takayanagi, H. Contribution of nuclear factor of activated T cells c1 to the transcriptional control of immunoreceptor osteoclast-associated receptor but not triggering receptor expressed by myeloid cells-2 during osteoclastogenesis. *J. Biol. Chem.* **2005**, *280*, 32905–32913.
- (14) Asagiri, M.; Takayanagi, H. The molecular understanding of osteoclast differentiation. *Bone* **2007**, *40*, 251–264.
- (15) Yagi, M.; Miyamoto, T.; Sawatani, Y.; Iwamoto, K.; Hosogane, N.; Fujita, N.; Morita, K.; Ninomiya, K.; Suzuki, T.; Miyamoto, K.; Oike, Y.; Takeya, M.; Toyama, Y.; Suda, T. DC-STAMP is essential for cell–cell fusion in osteoclasts and foreign body giant cells. *J. Exp. Med.* **2005**, *202*, 345–351.
- (16) Kukita, T.; Wada, N.; Kukita, A.; Kakimoto, T.; Sandra, F.; Toh, K.; Nagata, K.; Iijima, T.; Horiuchi, M.; Matsusaki, H.; Hieshima, K.; Yoshie, O.; Nomiyama, H. RANKL-induced DC-STAMP is essential for osteoclastogenesis. *J. Exp. Med.* **2004**, *200*, 941–946.
- (17) Grigoriadis, A. E.; Wang, Z. Q.; Cecchini, M. G.; Hofstetter, W.; Felix, R.; Fleisch, H. A.; Wagner, E. F. c-Fos: A key regulator of osteoclast-macrophage lineage determination and bone remodeling. *Science* **1994**, *266*, 443–448.
- (18) Wada, T.; Nakashima, T.; Hiroshi, N.; Penninger, J. M. RANKL–RANK signaling in osteoclastogenesis and bone disease. *Trends Mol. Med.* **2006**, *12*, 17–25.
- (19) Watts, N. B. Bisphosphonate treatment of osteoporosis. *Clin. Geriatr. Med.* **2003**, *19*, 395–414.
- (20) Strampel, W.; Emkey, R.; Civitelli, R. Safety considerations with bisphosphonates for the treatment of osteoporosis. *Drug Saf.* **2007**, *30*, 755–763.
- (21) Conte, P.; Guarneri, V. Safety of intravenous and oral bisphosphonates and compliance with dosing regimens. *Oncologist* **2004**, *9* (Suppl. 4), 28–37.
- (22) Soekanto, A.; Ohya, K.; Ogura, H. The effect of sodium salicylate on the osteoclast-like cell formation and bone resorption in a mouse bone marrow culture. *Calcif. Tissue Int.* **1994**, *54*, 290–295.
- (23) Tsai, H. Y.; Lin, H. Y.; Fong, Y. C.; Wu, J. B.; Chen, Y. F.; Tsuzuki, M.; Tang, C. H. Paeonol inhibits RANKL-induced osteoclastogenesis by inhibiting ERK, p38 and NF- κ B pathway. *Eur. J. Pharmacol.* **2008**, *588*, 124–133.
- (24) Hsu, Y. C.; Cheng, C. P.; Chang, D. M. *Plectranthus amboinicus* attenuates inflammatory bone erosion in mice with collagen-induced arthritis by downregulation of RANKL-induced NFATc1 expression. *J. Rheumatol.* **2011**, *38*, 1844–1857.
- (25) Cheng, C. P.; Huang, H. S.; Hsu, Y. C.; Sheu, M. J.; Chang, D. M. A benzamide-linked small molecule NDMC101 inhibits NFATc1 and NF- κ B activity: A potential osteoclastogenesis inhibitor for experimental arthritis. *J. Clin. Immunol.* **2012**, *32*, 762–777.
- (26) Idris, A. I.; Mrak, E.; Greig, I.; Guidobono, F.; Ralston, S. H.; van't Hof, R. ABD56 causes osteoclast apoptosis by inhibiting the NF κ B and ERK pathways. *Biochem. Biophys. Res. Commun.* **2008**, *371*, 94–98.
- (27) van't Hof, R. J.; Idris, A. I.; Ridge, S. A.; Dunford, J.; Greig, I. R.; Ralston, S. H. Identification of biphenylcarboxylic acid derivatives as a novel class of bone resorption inhibitors. *J. Bone Miner. Res.* **2004**, *19*, 1651–1660.
- (28) Steffen, J. D.; Coyle, D. L.; Damodaran, K.; Beroza, P.; Jacobson, M. K. Discovery and structure–activity relationships of modified salicylanilides as cell permeable inhibitors of poly(ADP-ribose) glycohydrolase (PARG). *J. Med. Chem.* **2011**, *54*, 5403–5413.
- (29) Brown, M. E.; Fitzner, J. N.; Stevens, T.; Chin, W.; Wright, C. D.; Boyce, J. P. Salicylanilides: Selective inhibitors of interleukin-12p40 production. *Bioorg. Med. Chem.* **2008**, *16*, 8760–8764.
- (30) Liu, F. C.; Huang, H. S.; Huang, C. Y.; Yang, R.; Chang, D. M.; Lai, J. H.; Ho, L. J. A benzamide-linked small molecule HS-Cf inhibits TNF- α -induced interferon regulatory factor-1 in porcine chondrocytes: A potential disease-modifying drug for osteoarthritis therapeutics. *J. Clin. Immunol.* **2011**, *31*, 1131–1142.
- (31) Coste, E.; Greig, I. R.; Mollat, P.; Rose, L.; Gray, M.; Ralston, S. H.; van't Hof, R. J. Identification of small molecule inhibitors of RANKL and TNF signalling as anti-inflammatory and antiresorptive agents in mice. *Ann. Rheum. Dis.* **2013**, DOI: 10.1136/annrheumdis-2013-203700.
- (32) Crockett, J. C.; Rogers, M. J.; Coxon, F. P.; Hocking, L. J.; Helfrich, M. H. Bone remodelling at a glance. *J. Cell Sci.* **2011**, *124*, 991–998.
- (33) Bellows, C. G.; Aubin, J. E.; Heersche, J. N. Initiation and progression of mineralization of bone nodules formed in vitro: The role of alkaline phosphatase and organic phosphate. *Bone Miner.* **1991**, *14*, 27–40.
- (34) Quarles, L. D.; Yohay, D. A.; Lever, L. W.; Caton, R.; Wenstrup, R. J. Distinct proliferative and differentiated stages of murine MC3T3-E1 cells in culture: An in vitro model of osteoblast development. *J. Bone Miner. Res.* **1992**, *7*, 683–692.
- (35) Wang, D.; Christensen, K.; Chawla, K.; Xiao, G.; Krebsbach, P. H.; Franceschi, R. T. Isolation and characterization of MC3T3-E1 preosteoblast subclones with distinct in vitro and in vivo differentiation/mineralization potential. *J. Bone Miner. Res.* **1999**, *14*, 893–903.
- (36) Skala, P.; Machacek, M.; Vejsova, M.; Kubicova, L.; Kunes, J.; Waisser, K. Synthesis and antifungal evaluation of hydroxy-3-phenyl-

2H-1,3-benzoxazine-2,4(3H)-diones and their thioanalogs. *J. Heterocycl. Chem.* **2009**, *46*, 873–880.

(37) Alam, M. I.; Gomes, A. Viper venom-induced inflammation and inhibition of free radical formation by pure compound (2-hydroxy-4-methoxy benzoic acid) isolated and purified from anantamul (*Hemidesmus indicus* R. BR) root extract. *Toxicol.* **1998**, *36*, 207–215.

(38) Hayman, A. R.; Jones, S. J.; Boyde, A.; Foster, D.; Colledge, W. H.; Carlton, M. B.; Evans, M. J.; Cox, T. M. Mice lacking tartrate-resistant acid phosphatase (Acp 5) have disrupted endochondral ossification and mild osteopetrosis. *Development* **1996**, *122*, 3151–3162.

(39) Saftig, P.; Hunziker, E.; Everts, V.; Jones, S.; Boyde, A.; Wehmeyer, O.; Suter, A.; von Figura, K. Functions of cathepsin K in bone resorption—Lessons from cathepsin K deficient mice. *Adv. Exp. Med. Biol.* **2000**, *477*, 293–303.

(40) Xia, L. H.; Kilb, J.; Wex, H.; Li, Z. Q.; Lipyansky, A.; Breuil, V.; Stein, L.; Palmer, J. T.; Dempster, D. W.; Bromme, D. Localization of rat cathepsin K in osteoclasts and resorption pits: Inhibition of bone resorption and cathepsin K-activity by peptidyl vinyl sulfones. *Biol. Chem.* **1999**, *380*, 679–687.

(41) Ishibashi, O.; Niwa, S.; Kadoyama, K.; Inui, T. MMP-9 antisense oligodeoxynucleotide exerts an inhibitory effect on osteoclastic bone resorption by suppressing cell migration. *Life Sci.* **2006**, *79*, 1657–1660.

(42) Delaisse, J. M.; Andersen, T. L.; Engsig, M. T.; Henriksen, K.; Troen, T.; Blavier, L. Matrix metalloproteinases (MMP) and cathepsin K contribute differently to osteoclastic activities. *Microsc. Res. Technol.* **2003**, *61*, 504–513.

(43) Miyazaki, T.; Katagiri, H.; Kanegae, Y.; Takayanagi, H.; Sawada, Y.; Yamamoto, A.; Pando, M. P.; Asano, T.; Verma, I. M.; Oda, H.; Nakamura, K.; Tanaka, S. Reciprocal role of ERK and NF- κ B pathways in survival and activation of osteoclasts. *J. Cell Biol.* **2000**, *148*, 333–342.

(44) Shiotani, A.; Takami, M.; Itoh, K.; Shibasaki, Y.; Sasaki, T. Regulation of osteoclast differentiation and function by receptor activator of NF κ B ligand and osteoprotegerin. *Anat. Rec.* **2002**, *268*, 137–146.

(45) Yamashita, T.; Yao, Z.; Li, F.; Zhang, Q.; Badell, I. R.; Schwarz, E. M.; Takeshita, S.; Wagner, E. F.; Noda, M.; Matsuo, K.; Xing, L.; Boyce, B. F. NF- κ B p50 and p52 regulate receptor activator of NF- κ B ligand (RANKL) and tumor necrosis factor-induced osteoclast precursor differentiation by activating c-Fos and NFATc1. *J. Biol. Chem.* **2007**, *282*, 18245–18253.

(46) Asagiri, M.; Sato, K.; Usami, T.; Ochi, S.; Nishina, H.; Yoshida, H.; Morita, I.; Wagner, E. F.; Mak, T. W.; Serfling, E.; Takayanagi, H. Autoamplification of NFATc1 expression determines its essential role in bone homeostasis. *J. Exp. Med.* **2005**, *202*, 1261–1269.

(47) Ishida, N.; Hayashi, K.; Hoshijima, M.; Ogawa, T.; Koga, S.; Miyatake, Y.; Kumegawa, M.; Kimura, T.; Takeya, T. Large scale gene expression analysis of osteoclastogenesis in vitro and elucidation of NFAT2 as a key regulator. *J. Biol. Chem.* **2002**, *277*, 41147–41156.

(48) Zhu, Z. W.; Shi, L.; Ruan, X. M.; Yang, Y.; Li, H. Q.; Xu, S. P.; Zhu, H. L. Synthesis and antiproliferative activities against Hep-G2 of salicylanide derivatives: Potent inhibitors of the epidermal growth factor receptor (EGFR) tyrosine kinase. *J. Enzyme Inhib. Med. Chem.* **2011**, *26*, 37–45.

(49) Denizot, F.; Lang, R. Rapid colorimetric assay for cell growth and survival. Modifications to the tetrazolium dye procedure giving improved sensitivity and reliability. *J. Immunol. Methods* **1986**, *89*, 271–277.